Molecular identification and functional analysis of HrpZ2, a new member of harpin superfamily from *Pseudomonas syringae* inducing hypersensitive response in tobacco.

Kishori Lal[1], Anurag Joshi[1], Vartika Saini[1], Mujahid Mohammed[2], P.V.S.R.N Sarma[3], Debashish Dey[1*]

[1]Laboratory of Plant Biotechnology, School of Biotechnology, Banaras Hindu University, Varanasi, UP, PIN-221005, India

[2]Department of Botany, Bharathidasan Government College for Women, Affiliated to Pondicherry University, Puducherry, India

[3]Department of Plant Sciences, University of Hyderabad, Hyderabad-500046, Telangana, India

*** Correspondence: Dr. Debashish Dey**
Corresponding Author
debashish@bhu.ac.in, deybiotech@gmail.com

Keywords: Hypersensitive response, harpin, *Pseudomonas syringae*, plant-microbe, ROS, systemic acquired resistance.

Running title: **Characterization of novel harpin-induced hypersensitive response**

Abstract

Harpins belong to a group of proteins with distinctive features such as heat stability, glycine richness, and absence of cysteine. Harpins are secreted by many gram-negative phytopathogens *via* the type III secretion system and are known for their ability to trigger hypersensitive response followed by induction of systemic acquired resistance in non-host plants. However, there is lack of studies on exploring the mechanism of action of harpins. In this study, we report cloning of a novel harpin gene (HrpZ2) from *Pseudomonas syringae* strain MTCC-11950, belonging to harpin superfamily. *In silico* analysis revealed that about 50.29% of the protein consists of alpha-helices, 48.53% are random coils, and only 1.16% are beta-sheets, and nearly half (42%) of the protein consists of intrinsically disordered regions. Based on a prokaryotic predictive model and the presence of a signal peptide on its N-terminus, the subcellular localization of harpin is predicted as extracellular. Determination of protein sequence and structure are fundamental to understanding its biological function. To date, no experimentally determined crystal structure of any harpin protein is available. Using this information, we built and validated an *ab initio* model (with 99% of residues in allowed/additionally allowed regions and a Z-score of -5.3) of harpin. Phylogenetic analysis and functional domain studies revealed that this novel harpin belongs to the harpin superfamily. Infiltration of harpin in tobacco leaves resulted in hypersensitive response, which was associated with oxidative burst, callose

deposition, localized cell death, and increased activity of defense-related enzymes such as phenylalanine ammonia-lyase and polyphenol oxidase. Furthermore, infiltration of harpin in non-host plants from different angiosperm families induced hypersensitive response, indicating broad-spectrum agricultural applicability of this novel harpin protein. Current study sheds light on the molecular and functional analysis of novel harpin protein and its ability to induce HR response in broad range of non-host plants.

1 Introduction

The interaction between plants and phytopathogens is shaped by a dynamic and continuous co-evolutionary process. Phytopathogens deploy diverse strategies to suppress host defenses and establish infection, while plants, in turn, have evolved a multilayered immune system to detect and restrict invading pathogens (Jones and Dangl, 2006; Cui et al., 2015). This innate immune system is broadly categorized into two hierarchical layers: PAMP triggered immunity (PTI) and effector triggered immunity (ETI).

The first layer, PTI involves the recognition of the pathogen's surface molecular patterns known as pathogen-associated molecular patterns (PAMP) by plant plasma membrane-bound receptors defined as pattern recognition receptors (PRR). Usually, PAMPs are considered to be essential for general microbial fitness and survival. These PAMP-PRR complexes activate the immune responses termed as PAMP-triggered immunity (PTI) in plants (Zipfel et al., 2006; Dodds et al., 2010). However, adapted pathogens have evolved the capacity to overcome PTI-mediated immunity through deployment of effector proteins into the host cytoplasm *via* specialized secretion systems, notably the Type-III secretion system (T3SS) in gram negative bacteria resulting in effector-triggered susceptibility (ETS) (Faris et al., 2010). These effectors target the host signaling and contribute to the virulence of invading pathogens. On the other side, plants got evolved parallelly and acquired more receptors that specifically recognize and bind to the pathogen effectors and mount a second layer of defense response known as effector-triggered immunity (ETI). The ETI leads to an immediate oxidative burst (ROS) followed by the hypersensitive response (HR) mediated cell death of plant cells at and near the sites of pathogen invasion. HR was first time reported by Wei et al. 1992, characterized by the rapid, highly localized defense response that is generally considered a form of programmed cell death (PCD) in plants followed by the induced systemic acquired resistance (SAR), a salicylic acid (SA)-dependent defense response throughout the plant which is effective against a wide spectrum of phytopathogens (Ricci 1997).

Plant-microbe interaction is a multifaceted phenomenon that has been explored for decades, and still there are lot to be known. In the current scenario, significant progress has been made in identifying and characterizing broad spectrum defense response elicitors that can boost plant immunity (Mandal et al., 2013). These elicitors might be derived from microbial, fungal, or viruses, and function as molecular signals that trigger innate immune responses such as oxidative burst, hypersensitive response mediated programmed cell death, accumulation of callose, lignification, pathogenesis-related (PR) proteins, and the activation of key defense enzymes like polyphenol oxidase (PPO) and phenylalanine ammonia-lyase (PAL), offering a promising alternative to traditional chemical pesticides (Choi et al., 2012; Lavanya et al., 2022; Zhu et al., 2024).

Certain gram-negative, plant-pathogenic bacteria harbor pathogenicity (*hrp*) gene clusters that regulate HR in nonhost plants or resistant cultivars of host plants and control the pathogenicity in susceptible plants (Collmer et al., 1998). Generally, the *hrp* cluster contains genes that encode the components of a bacterial type III secretion system, through which the effector proteins are injected and delivered into the host's cytosol (Hueck 1998; Galán and Collmer, 1999). Study on the *hrp* gene cluster of *X. oryzae* pv. *oryzae*, which encodes a specific protein transport system (type III secretion

This is a provisional file, not the final typeset article

system) and is made up of nine *hrp* and nine *hrc* (*hrp* conserved) while eight *hpa* (*hrp*-associated) genes. HrpG and HrpX are the regulators of the *hrp* gene cluster because they controlled all these genes (Choi et al., 2008). The nine *hrp* genes that are highly conserved among pathogenic bacteria that contained type III secretion systems were renamed as *hrp*-conserved (*hrc*) genes (Bogdanove et al.,1996; Wei et al., 2000). In *Pseudomonas syringae*, it was shown that two families of proteins are secreted by the Hrp secretion system: Avr proteins encoded by the virulence (*avr*) gene of the pathogen and harpins, like HrpZ and HrpW, etc. Harpin (*hrpN*) was first identified by Wei et al. (1992) from the *Erwinia amylovora* and named as $Harpin_{Ea}$. To date, several other *hrp*-encoded harpin elicitors have been identified from various phytopathogenic bacteria collectively termed as Harpin protein family (Choi et al, 2012; He et al., 1993; Li et al., 2011). Recently, all these harpins were classified into five major groups based on their inherent domain structure and protein similarity, *viz*., HrpN group (from *Erwinia* spp.), HrpZ1 group (from *Pseudomonas syringae*), HrpW1 (from *Erwinia* spp., *Pseudomonas syringae*, *Ralstonia* spp.), Hpa1 group and its orthologs (from *Xanthomonas* spp.), and 'Others' group contained remaining unclassified harpin proteins (Choi et al., 2013). The HrpZ-group of harpins are a major T3SS□dependent proteins secreted by *P. syringae* which shares some common characteristics with other groups of harpins: such as they are glycine-rich, lack of cysteine (exception Hpa1), very few aromatic amino acids and high thermal stability (Choi et al., 2013; Tarafdar et al., 2009). To investigate the thermal activity of the harpin, few studies have been carried out such as boiling the harpin protein for 10 min. Although it is still unclear as what is the highest temperature they can tolerate while retaining its active and how long they can withstand such temperatures. The reason behind the high thermal stability of harpin proteins might be due to its inherent structural features rendering thermostability, it is still unknown and yet to be explored (Tarafdar et al., 2009). A recent study on the thermal stability of harpins showed that the harpin (HpaXpm) remains active at 100°C, 150°C, or 200°C while the ability of heat-treated harpins to HR induction varied with respect to temperature (Liu et al., 2020). Harpins can act as an elicitor to elicit a HR associated with systemic acquired resistance (SAR) and provide diverse benefits to the plants such broad-spectrum durable disease resistance, quality, and yield improvement in crops. Harpin (HrpN) protein from *Erwinia amylovora*, enhances drought resistance in *Arabidopsis thaliana* by activating the abscisic acid (ABA)-dependent signalling pathways (Dong et al., 2005). Similarly, harpin (HrpZ) from *Pseudomonas* spp., has been reported to increase disease resistance in sugar beet (*Beta vulgaris*) and *Nicotiana benthamiana* against rhizomania disease caused by Beet necrotic yellow vein virus (Pavli et al., 2011). Moreover, harpin proteins have also been involved in ethylene-mediated resistance against insect herbivory and promoting over all plant growth and vigour (Chuang et al., 2010; Miao et al., 2019). Recent reports (Li et al., 2015) showed that aquaporin proteins present on the plasma membranes act as receptors for the interaction of extracellular $harpin_{Xoo}$ proteins. Recent reports from our lab predicted a signature sequence present in the aquaporin protein and the potential interacting amino acid residues involved in the harpin-aquaporin interaction through *in silico* docking studies (Lal et al., 2023).

In summary, these findings demonstrate that harpins can elicit a wide range of physiological and defence responses in non-host plants. Given their potential in enhancing both biotic and abiotic stress tolerance, harpins represent as a promising tool for sustainable crop management. To maximize their agricultural utility, it is essential to identify and screen new harpin proteins with superior elicitor activity and broader applicability for crop improvement.

In the present study, we report the molecular and functional characterization of *hrpZ2*, a newly identified member of the harpin superfamily of type III secretion system effectors from *P. syringae*. The harpin gene encodes a 34.5 kDa predicted protein, exhibiting characteristic features of harpins, including a glycine-rich sequence and a potential secondary structure formation. Functional

assays were conducted to assess its ability to induce HR in non-host plants, and activate defense-related signaling pathways and enhance plant growth to ascertain their bio-stimulant potential and use in agricultural applications.

2 Materials and methods

2.1 Plants, bacterial strains, and growth conditions

The seeds of tobacco plants (*Nicotiana tabacum* cv. xanthi) were maintained in the Laboratory of Plant Biotechnology at 4°C. For this study, tobacco seeds were sown in flat plastic trays (32 x 15 cm) containing a 1:1:1(v/v) mixture of vermiculite, garden soil and sand. Later, the germinal seedlings (four-leafed stage) plants were transplanted individually into 12 x 10 cm plastic pots (one plant per pot). Tobacco plants were maintained under laboratory conditions at 23 ± 3°C, with a 16 h light and 8 h dark photoperiod.

Harpin gene was amplified from *Pseudomonas syringae* strain MTCC-11950, obtained from the Microbial Type Culture Collection and Gene Bank (MTCC), Chandigarh, India. Recombinant expression of the harpin protein was carried out using *Escherichia coli* DH5α cells cultured on Luria-Bertani (LB) Agar (Himedia, M1151) and Luria-Bertani (LB) broth (Himedia, M1245) at 37°C. Kanamycin was used at a final concentration of 50 µg/mL for selection.

2.2 NCBI Submission of the harpin gene

The harpin gene was amplified from *P. syringae* (MTCC-11950). DNA sequence analysis revealed that it is a previously uncharacterized member of the harpin protein superfamily. The nucleotide sequence was submitted to the NCBI GenBank database under the accession number, GenBank ID: OQ338148.1. (https://www.ncbi.nlm.nih.gov/nuccore/OQ338148).

2.3 *In silico* analysis of the primary, secondary and tertiary structures of harpin

2.3.1 Sequence retrieval and sequence-based analysis

The amino acid sequence of harpin was retrieved from National Centre for Biotechnology information (NCBI) GenBank: OQ338148.1, in the FASTA format. The physiochemical properties of harpin were analyzed using ProtParam tool (https://web.expasy.org/protparam/). Hydropathicity or hydrophobicity, isoelectric point (pI), instability index and molecular weight of harpin sequence were analyzed using Grand Average of Hydropathicity (GRAVY) web server. The PrDOS server (https://prdos.hgc.jp/cgi-bin/top.cgi) (Ishida and Kinoshita, 2007) was used to evaluate the disorderliness.

2.3.2 *Ab initio* modelling of harpin

Currently, there is no experimentally concluded tertiary structure available for harpin (GenBank ID of protein: WDY61303.1) in the Protein Data Bank (PDB). Consequently, the tertiary structure of the protein was modeled by utilizing I-TASSER server (https://zhanggroup.org/I-TASSER/) (Zheng et al., 2025). The tools such as VERIFY 3D (Colovos and Yeates, 1993), ERRAT (Bowie, J U et al., 1991), and PROCHECK (Laskowski et al., 1996) of the SAVES v.6.0 server (https://saves.mbi.ucla.edu) were used to analyze the Ramachandran Plot and validate the computationally predicted 3D structure. Z-score was calculated using ProSA (https://prosa.services.came.sbg.ac.at/prosa.php).

This is a provisional file, not the final typeset article

2.3.3 Functional domain prediction and analysis of domain architecture

The conserve domains (CD) study was done using the CD search tool of NCBI platform (https://www.ncbi.nlm.nih.gov). To detect and annotate the harpins' domains, a useful biological web server called PSIPRED (Cozzetto et al. 2016) was used. It predicts the functional domains in the secondary structure of proteins. The transmembrane helix packing and orientations of proteins in the membranes were predicted through PSIPRED workbench, the MEMPACK alpha-helical transmembrane protein structure prediction server (Nugent et al., 2011). The helix and loop regions were predicted using the MEMSAT-SVM algorithms, and their orientations were confirmed by kyte-doolittle method in the TMHMM web server of PSIPRED Workbench (Nugent and Jones, 2009).

2.3.4 Evolutionary study of Harpin

The evolutionary history was inferred using the Maximum Likelihood (ML) method, and the phylogenetic tree was constructed by MEGA11.0 software. Bootstrap analysis with 1000 replicates was performed to ensure statistical robustness and reliability of the branching patterns. The phylogenetic analysis was done among 48 harpin proteins derived from several bacterial genera: *Xanthomonas, Pseudomonas, Ralstonia, Erwinia, Rhizobium, Dickeya,* and *Pectobacterium.* The phylogenetic tree was be visualized on the iTOL online tool (https://itol.embl.de/shared/2PuqbCYlUfiSH) (Letunic and Bork, 2024).

2.3.5 Subcellular localization of harpin

The subcellular localization of harpin protein was predicted using DeepLocPro - 1.0. The server predicted the subcellular localizations using the prokaryotic predictive model. It provides the prediction probability for different subcellular compartments like outer membrane, periplasmic space, cell wall and surface, cytoplasmic membranes based on the amino acid sequence of the signal sequence of the protein.

2.4 Cloning, expression, and purification of harpin

To construct recombinant plasmids encoding poly-histidine-tailed harpin fusion protein, initially, the harpin gene was amplified from the genomic DNA of *Pseudomonas syringae* strain (MTCC-11950). The harpin gene (1.03 kb) encoding harpin was cloned in *pET28a* vector (maintained in our laboratory) under the *Nde*I and *Xho*I restriction sites. The recombinant plasmids (*pET28a-hrpZ*) were transformed into *E.coli* BL21 (DE3) expression host and grown in LB broth supplemented with Kanamycin (50 µg/ml) till the OD_{600nm}~ 0.5 and the synthesis of harpin protein was induced with 0.001 M Isopropyl-β-D-thiogalactopyranoside (IPTG) at 37°C for 3 h with shaking conditions (200 rpm). The bacterial cells were harvested using centrifugation at 6000 rpm at 4°C and the pellet was resuspended in 10 mM sodium phosphate buffer (pH 7.5) supplemented with 1 mg/ml lysozyme and immediately sonicated using probe sonicator (Labman, 3 mm probe) using pulse rate of 30 s and 20 s on/off respectively, with 40% amplitude, for 20 minutes with two minutes interval to cool down. The sonicated lysate was centrifuged at 11,000 rpm for 30 min and the supernatant was loaded onto a nickel-nitrilotriacetic acid (Ni-NTA, Qiagen, USA) affinity chromatography column filled with Ni-NTA slurry. The protein was purified following the manufacturer's protocol (Manual purification of 6xHis-tagged proteins from *E. coli*, Qiagen) with some modifications. The targeted, 6x his-tagged harpin proteins from crude protein bind with nickel inside the column, followed by a wash to remove the unwanted or loosely attached proteins in the column using washing buffer (sodium phosphate buffer (10 mM, pH 7.5) with 20 mM and 30 mM imidazole). Finally, the targeted harpin protein was eluted out using elution buffer (sodium phosphate buffer (10 mM, pH 7.5) with 200 mM imidazole). The purified protein was extensively dialyzed using dialysis membrane tubing

(10 kDa cut off, SnakeSkin™ Dialysis Tubing, Thermo Scientific™, USA) against 10 mM sodium phosphate buffer (pH 7.5) without imidazole. The dialyzed protein was concentrated using an amicon centrifuge column (10 kDa cut-off, Millipore, USA). The purity of the protein was checked by running on a 12% SDS-PAGE gel. The estimation of protein concentration was done by following standard Bradford's method (Bradford 1976).

2.5 SDS-PAGE and western blotting of harpin (HrpZ2)

For western blotting, the protein was resolved on a 12% SDS-PAGE gel under reducing conditions along with a molecular weight marker and then transferred to a polyvinylidene difluoride (PVDF) membrane. The membrane was blocked with a blocking buffer containing 5% (w/v) non-fat milk in Tris Buffered Saline with Tween 20 (TBS, 150 mM NaCl and 0.05% Tween 20, pH 7.4) at room temperature for one hour, followed by incubation with harpin primary anti-His-tag antibody diluted 1:5000 in 1X TBST with 5% milk, incubated at 4°C with gentle shaking for overnight. Further, the PVDF membrane was washed five times with TBST for 10 min each time. The membrane was then incubated with goat anti-rabbit IgG-ALP conjugated secondary antibody in TBST (1:2000) at room temperature for 1 h and washed five times with TBST for 10 min each time. Finally, the immunoblot was visualized on the PVDF membrane using BCIP-NBT substrate for alkaline phosphatase.

2.6 Determination of the effective concentration of harpin protein to elicit HR in tobacco.

Tobacco plants (*Nicotiana tabacum* cv. xanthi) were grown under laboratory conditions at 23 ± 3°C, with a photoperiod of 16 h light and 8 h dark (Li, Y.R et al. 2013). For this study, five-week-old plants were used for infiltration with purified harpin (HrpZ2). To assess the elicitation of hypersensitive response (HR), the harpin protein was diluted in 10 mM sodium phosphate buffer (pH 7.5) to a final concentration (30 µg/mL). Infiltration was carried into the abaxial surface of the third to fifth leaves from the top using a 1 mL needless sterile syringe. Sodium phosphate buffer (10 mM, pH 7.5) was used as a negative control.

2.7 Host range determination of harpin protein using HR-induction assay.

Harpins are proteinaceous elicitor well documented for their role in inducing plant defense responses, particularly through the elicitation of the hypersensitive response (HR). To evaluate the host-range of new member of harpin elicitor derived from *P. syringae*, we assessed its ability to trigger localized HR in various angiosperm plant families. Affinity purified harpin protein was diluted in 10 mM sodium phosphate buffer (pH 7.5) to a final concentration of 50 µg/mL and infiltrated into the abaxial (lower) surface of the leaves of 12 non-host plants belonging to eight angiosperm plant families. A sterile needless syringe (1 mL) was used for the infiltration. Each leaf was infiltrated on one half with the purified harpin protein, while the opposite half was infiltrated with sodium phosphate buffer (10 mM, pH 7.5) as a negative control. Leaves were observed and photographed at different time intervals: before infiltration, and at 0, 12, 18, 24, 30 and 48 h post infiltration. A final observation and a photograph were taken five days post infiltration. A clear localized colourless zone of dead cells, indicative of hypersensitive response was observed in the harpin treated areas (Fig. 8). The onset and intensity of HR varied among different plant species.

2.8 Biochemical assays

This is a provisional file, not the final typeset article

2.8.1 Detection of reactive oxygen species (H_2O_2)

Hydrogen peroxide (H_2O_2) is an important signal molecule in plant defense pathway, and its accumulation in plant tissues can be detected using 3, 3'-diaminobenzidine dyes (DAB, a histochemical reagent for H_2O_2 detection). Detection of hydrogen peroxide (H_2O_2) was done using the method given by Daudi and O'Brien, 2012. Harpin from *Pseudomonas syringae* was syringe infiltrated into the interveinal region of abaxial side of the plants leaves. A needless sterile syringe (1 mL) is used to infiltrate the purified harpin protein (final concentration of 30 µg/ml) into the fully expended third to fourth tobacco leaves. Sodium phosphate buffer (10 mM, pH 7.5) was used as a negative control. The H_2O_2 was detected by following the method of Daudi et al. (2012) with some modifications. For the detection of H_2O_2 accumulation, 1 mg/ml DAB (Himedia, RM2735) solution was prepared in 10 mM sodium phosphate (Na_2HPO_4) buffer with 0.05% (v/v) Tween 20, adjusted to pH 3.8 with conc. HCL. The harpin treated leaves were harvested at 6, 12, and 24 hours post infiltration (hpi) and soaked in DAB-HCL solution (pH 3.8) for 10 hours at room temperature in dark conditions followed by boiling in bleaching solution (ethanol: acetic acid: glycerol in a 3:1:1, v/v/v ratio) for 15 minutes. The entire chlorophyll was bleached out and a red, brown precipitate resulting from DAB's reaction with hydrogen peroxide was visualized under light microscope and photographed. Each experiment was carried out 3 times, and each of them contained 6 leaves from different plants. ROS signals were also observed in harpin treated tobacco leaf tissue by submerging in 10 µM 2′,7′–dichlorofluorescin diacetate (DCFDA, SIGMA-Aldrich, D6883-50MG) solution in 10 mM sodium phosphate buffer (pH 7.5) and incubated in dark for 20 min at room temperature. Sample tissues were gently washed with 10 mM sodium phosphate buffer (pH 7.5) and mounted on glass slide and ROS signals were observed using fluorescence microscope (Nikon, Japan).

2.8.2 Quantification of Hydrogen peroxide using FOX method

Quantification of hydrogen peroxide (H_2O_2) was done using FOX (Ferrous oxidation in xylenol orange) method given by Jiang et al. (1990) with few modifications. The absorbance (560 nm) of colored complex formed due to the oxidation of Fe^{2+} to Fe^{3+} by H_2O_2 and binding of the resulting Fe^{3+} to xylenol orange was measured. Briefly, the FOX reagent (250 µM ferrous ammonium sulphate $(NH_4)_2Fe(SO_4)_2.6H_2O$, 100 µM xylenol orange, 25 mM H_2SO_4, and 100 mM sorbitol) was prepared by taking about 80 mL of 25 mM H_2SO_4 and 9.8 mg ammonium ferrous sulphate, 7.6 mg xylenol orange, and 1.82 g sorbitol were added and mix thoroughly until the sorbitol was completely dissolved, and the volume was increased to 100 mL with 25 mM H_2SO_4. After different time intervals including 0, 3, 6, 9, 12, 24, 48 and 72-hour post infiltration (hpi), 0.5 g leaf samples were ground in liquid nitrogen and suspended in 5 mL ice cold 0.1% trichloroacetic acid (TCA) solution. Supernatant was separated by centrifugation at 13,000 rpm for 25 min at 4°C. Sample was prepared by mixing 0.5 ml of FOX reagent and 0.5 ml of leaf extract (supernatant) and incubated in dark for 30 minutes in room temperature. The absorbance was measured by spectrophotometer at 560 nm. The H_2O_2 was used as standards. Results were expressed in µmol H_2O_2 per gram fresh weight (µmol/g FW).

Calculations: H_2O_2 content = C × (V/W)

Where:

C = concentration from standard curve (µM),

V = extraction volume (mL),

W = tissue weight (g)

2.8.3 Cell death estimation by using trypan blue staining

For the detection of dead cells in harpin treated tobacco leaves, trypan blue staining was performed as described by Koch & Slusarenko (1990). The leaves were detached at 24, 48 and 72 hpi and boiled in lactophenol trypan blue solution containing (lactic acid (10 mL), glycerol (10 mL), trypan blue (7.6 mg) and (10 ml) phenol mixed in 10 mL distilled water). Full (uncut) leaves were boiled for approximately 1 min in the staining solution and then decolorized by using clearing solution (mixing 3 parts ethanol (96%) with 1-part acetic acid) (For 100 mL solution: 75 mL ethanol (96%), 25 mL glacial acetic acid). The leaves were stained at room temperature for 3-4 hours; the solution was replaced three times until tissue becomes transparent. The de-stained leaves were rinsed with distilled water followed by mounting in 60% glycerol and covering with coverslip carefully and photographed using light microscope (Magnus Opto Systems India Pvt. Ltd.).

2.8.4 Detection of callose deposition

Accumulation of callose was detected by following the protocol given by Luna et al. (2011) with some modifications. To visualize callose accumulation, leaves of tobacco plants (six to eight leafed-stage) were syringe infiltrated at the abaxial surface without hypodermic needle. After 24-hpi, infiltrated leaf tissue was carefully excised followed by chlorophyll removal and the samples were completely dehydrated in ethanol (96%) by three-times repeated immersions. Specimens were rinsed briefly with distilled water followed by equilibration by incubating in sodium phosphate buffer (10 mM, pH 7.5) for 30 minutes at room temperature. Sufficient volume of aniline blue (0.05%) solution was added to stain the specimens and incubated in dark for 1 h at room temperature. The specimens were mounted on a microscopic slide using glycerol (50%) and covered with a coverslip. Mounted specimens were visualized under confocal laser scanning microscope (Zeiss, LSM780) with excitation wavelength of 405 nm and emission at 530 nm. Sodium phosphate buffer (10 mM, pH 7.5) was used as control. Callose intensity was calculated (using Image J software) by measuring blue pixels in the image and total pixels covering plant material. The results were normalized against the control treatment (set as unity). The data was compiled from at least three independent experiments. Means and standard deviations were calculated (Data not shown).

Calculation of ratio: (blue pixels)/ (total plant material pixels).

2.8.5 Determination of PAL Enzyme levels

Phenylalanine ammonia-lyase (PAL) activity was measured by following the protocol of Cheng & Breen (1991). PAL activity was measured by conversion of L-phenylalanine to trans-cinnamic acid. The harpin treated leaf was detached after different intervals including 2, 4, 12, 24 and 48 hpi and 0.5 g leaf tissue was homogenized in liquid nitrogen using a pre-chilled mortar and pestle, and resuspended into 5 ml of boric acid extraction buffer (0.05 M boric acid, 5 mM β-mercaptoethanol, 1 mM EDTA, and 0.05 g of polyvinylpyrrolidone). Supernatant was collected after centrifugation at 13000 rpm for 20 minutes at 4°C. Reaction mixture contains 500 µl of 50 mM boric acid buffer (pH 8.5), 200 µl of 50 mM L-phenylalanine (substrate), 200 µl of crude enzyme extract, 100 µl of distilled water and incubated at 37°C for 1 h. Reaction was stopped by adding 100 µl of TCA (10%). The absorbance at 290 nm was measured using spectrophotometer. The trans-cinnamic acid molar extinction coefficient (174000 $M^{-1}cm^{-1}$) was used to calculate PAL activity. The enzyme activity was expressed as the µmol of trans-cinnamic acid produced per minute per gram of fresh weight of leaf (µmol/min/g FW). The activity of the enzymes was assayed as described by Li et al. (2008) with few modifications.

Calculation:

This is a provisional file, not the final typeset article

PAL activity (μmol/min/g FW) = (ΔA290 × Volume of reaction mixture × Dilution factor) / (17400 × Time of incubation (min) × Weight of tissue (g))

Where: 17400 = Extinction coefficient of trans-cinnamic acid ($M^{-1}cm^{-1}$)

2.8.6 Determination of PPO enzyme levels

The enzymatic activity of PPO was examined by following the method reported by Chen et al., (2022) with few modifications. The PPO substrate catechol was added exogenously based on the protocol. The harpin infiltrated leaf samples were collected at different time intervals (i.e., 3, 6, 12, 24, 48, and 72 hours). The leaf sample (0.5 g) was ground and made into a fine powder using mortar and pestle, and resuspended into 3 mL extraction buffer (sodium phosphate buffer (100 mM) and 0.1 ml Triton X-100 (0.1% v/v), pH 6). The homogenate was transferred to a pre-chilled tube, followed by centrifugation after 30 min incubation (4°C) at 13000 rpm for 30 minutes at 4°C. The supernatant was used as the crude enzyme extract. Reaction mixture contained 1.9 ml of reaction buffer containing 10 mM catechol solution and 0.1ml of enzyme extract supernatant. The absorbance at 420 nm was measured at every 15-second for 5 minutes (For blank reaction buffer containing 10 mM catechol solution). One unit (U) of PPO activity was defined as the amount of enzyme that causes an increase in absorbance of 0.001 per minute under the assay conditions. PPO activity was determined using the formula:

PPO activity (U/g FW) = (ΔA□□□/min × Total volume × Dilution factor) / (ε × d × Volume of enzyme × Sample weight)

Where: ΔA□□□/min = Change in absorbance per minute, Total volume = Total reaction volume (2 ml), Dilution factor = Any dilution of the enzyme extract, ε = Molar extinction coefficient for quinone formation (24300 $M^{-1}cm^{-1}$ for benzoquione), d = Path length (1 cm), Volume of enzyme = Volume of extract used (0.1 ml), Sample weight = Fresh weight of leaf tissue (g).

3 Results

3.1 *In silico* analysis of the primary, secondary and tertiary structures of harpin

3.1.1 Analysis of physicochemical properties of harpin

The amino acid sequence of harpin was derived from NCBI data base (https://www.ncbi.nlm.nih.gov). Different physicochemical properties of harpin were examined using ProtParam tool of ExPASy server (Table 1). The theoretical pI (solution pH at which the net charge of an amino acid's surface is zero) (Gasteiger et al., 2005) and molecular weight of harpin are 4.93 and 34.5 kDa respectively. The aliphatic index was 85.99, and the instability index was 35.97 with a grand average of hydrophobicity (GRAVY) of -0.214. ProtParam tool computes the extinction coefficient (Table 1). The total number of positively charged residues such as Arg (R) and Lys (K), and the number of negatively charged residues such as Glu (D) and Asp (E), are 19 and 42 respectively.

3.1.2 Secondary structure of harpin

The harpin protein is predicted to be comprised of 50.29% (172 residues) alpha helices, 48.53% (166 residues) random coils and only 1.16 % (4 residues) beta sheet. Secondary structure of harpin protein was predicted by the web server PSIPRED and representative structure is shown in Fig. 1a. A total of 42 % (144 aa residues) of the total structure was predicted to be intrinsically disordered regions (Fig. 1b) (Jones 1999).

3.1.3 Prediction of the tertiary structure of harpin

The *ab-initio* model of harpin was prepared using I-TASSER web server, the computationally predicted model was validated employing VERIFY 3D, ERRAT, and PROCHECK tools of SAVES server by evaluating Ramachandran Plot (Fig. 2). The Ramachandran plot analysis revealed that 90.1 % of harpin residues reside in utmost favored area, 8.9 % are in additionally preferred regions, 0.4 % are in generously permitted regions while 0.7 % in disallowed area. About 282 residues are non-proline/non-glycine, 46 and 12 are of glycine and proline residues respectively. The 3D model of harpin was visualized using Discovery studio (BIOVIA).

3.1.4 Conserved domain analysis of harpin and transmembrane helix prediction

The annotation of evolutionary conserved domains of bacterial elicitor is an important move to understand the connection between DNA and protein and its biological function. The mapping of amino acid sequences of new identified harpin (HrpZ2) from *Pseudomonas syringae* showed that it specifically belongs to the harpin superfamily (Fig 3a). Proteins in this family play various roles such as to elicit HR in non-host plants and forming a cation permeable pore which play essential role in ion-conduction. A signal peptide is present at the N-terminal (from 1 to 23 residues) of the protein as detected by the MEMSAT-SVM method, whereas another region (from 323 to 338 residues) at the C-terminal forms a pore-lining helix while the residues from 24 to 322, form an extracellular loop confirmed as by the kyte-Doolittle method in TMHMM web server (Fig 3b).

3.1.5 Comparative domain analysis of harpins

The annotation of evolutionary conserved Choi et al., 2013, provided the 1st classification of harpins on the basis of presence or absence of functional domains. They predicted the functional domains in the secondary structure of each harpin using PSIPRED web server, and accordingly, they classified all the harpins into five groups based on the protein structures and similarity between them. In the present study, we also studied the domain analysis of our harpin (HrpZ2) along with each member from five different groups of harpins, based on Choi et al classification (2013), while considering few more additional input parameters such as the intrinsically disordered regions (IDRs) and number of glycines, cystines and leucines (Fig 4).

3.1.6 Subcellular localizations

The subcellular localizations of our harpin (HrpZ2) predicted using the DeepLocPro-1.0 server is graphically represented in figure 5 (Moreno et al., 2024). The graph of harpin is leveled with sorting signal importance, which represents the contribution of each amino acid residue of harpin protein to the prediction of its subcellular localization and the peaks of amino acid residues important for corresponding the protein to its predicted location. The subcellular location of harpin was primarily predicted as extracellular with a high probability (0.9915), showing a strong likelihood that the protein is located outside the cell. At the same time, alternative localizations were also predicted with very low probability. The alternative potential localizations are outer membrane (0.006) and periplasmic space (0.0023), while cell wall and surface, cytoplasmic membrane, and cytoplasmic predicted very low with 0.0001 probabilities.

3.1.7 Evolutionary study of harpins

Phylogenetic analysis of different harpins showed the sequence clustering which indicates a strong genus-specific grouping, with harpins from the same or closely related species forming tight clades. For instance, HrpN proteins from *Erwinia amylovora* formed a well-supported independent

This is a provisional file, not the final typeset article

clade (highlighted in red), reflecting a conserved evolutionary lineage distinct from other harpins. Similarly, harpins from *Pseudomonas syringae* pathovars, such as HrpZ, HrpW, and HopP1 showed broader distributions across several sub-branches (highlighted in green). Our harpin (HrpZ2) is marked with a red circle in the picture (Figure 6).

3.2 Cloning, expression, and purification of harpin

To clone, the harpin gene (*hrpZ2*, 1.03 kb) was successfully PCR amplified from *Pseudomonas syringae* (strain MTCC-11950) using a pair of primers 5'-CGAATCCCATATGCAGAGTCTCAGTCTTAAC – 3' (forward primer) and 5'-AGGATCCTCGAGGGCTGCAGCCTGATTGC – 3' (reverse primer). After cloning, recombinant plasmid (*pET28a-hrpZ*2) was confirmed by restriction digestion and transformed into *E. coli* BL21 cells to express the harpin protein. The harpin was effectively induced by 0.001 M IPTG at 37°C for 3 h with shaking condition (180 rpm). 6x-Harpin was purified by Ni-NTA affinity purification. The purity of the protein was checked by running on SDS-PAGE (12%) gel (34.5 kDa). The purified protein was extensively dialyzed (10 kDa cut off, Thermo Scientific™ SnakeSkin™ Dialysis Tubing) against 10 mM sodium phosphate buffer (pH 7.5). and was concentrated using an Amicon centrifuge column (10 kDa cut-off). The estimation of the protein concentration was done by following the Bradford's method (1976). The analysis of western blot shows that an anti-His tagged antibody specifically binds with his-tagged harpin protein (Fig. 7). This result verified that the recombinant harpin protein was successfully cloned, expressed, and purified.

3.3 Biochemical assays

3.3.1 Determination of range of non-host plants which responds with HR elicitation with harpin.

Purified harpin protein was infiltrated into the abaxial (lower) surface leaves of tobacco through a sterile needleless syringe. A clear visible HR was observed in localized area where the infiltration had happened while buffer treatment showed no such effect. Serial dilutions (1 µg/ml, 10 µg/ml, 20 µg/ml, 30 µg/ml, 40 µg/ml, and 50 µg/ml) of purified harpin protein were also similarly infiltrated into the abaxial surface of leaves of tobacco to identify the effective concentration required for the induction of HR, and the results revealed that the minimum concentration of the harpin elicitor required to elicit a visible HR was 30 µg/ml (Fig. 8).

Simultaneously, we were curious to know whether the harpin can elicit HR in various non-host plants of different angiosperm family or not. To study the HR elicitation, we tested 15 different non-host plants belonging to eight different angiosperm families including Solanaceae (*Solanum lycopersicum*, *Capsicum annuum* and *Solanum melongena*), Brassicaceae (*Brassica rapa* and *Brassica* sp.), Cucurbitaceae (*Cucumis sativus* and *Momordica charantia*), Caricaceae (*Carica papaya*), Fabaceae (*Glycine max*), Poaceae (*Zea mays*), Anacardiaceae (*Mangifera indica*) and Musaceae (*Musa* sp.). Sodium phosphate buffer (10 mM), pH 7.5 was used as a control. We observed that the onset and intensity of HR varied among the tested plants from different angiosperm families. Among them, *Momordica charantia* (Cucurbitaceae) exhibited the fastest HR response comparative to other plants with harpin infiltration. In contrast, plants such as *Musa* spp (Musaceae). *Carica papaya* (Caricaceae), and *Mangifera indica* (Annacardiaceae) exhibited a delayed development of macroscopic HR symptoms on their leaves. The bar graph (Fig. 8,D,i) represents the relative HR (cell death) development areas induced by infiltration with harpin protein. Each bar is color coded to correspond to a different plant species. Experiments were independently repeated at least three times, with five leaves used per plant. Data is presented as means ± standard deviation (SD).

3.3.2 ROS detection *via* DAB staining and DCFDA fluorescence

To study whether there was any ROS accumulation in the leaves treated with harpin or not, H_2O_2 level was recorded at several time points after infiltration of harpin into the leaves of tobacco. Harpin triggered rapid H_2O_2 accumulation in harpin infiltrated leaves (Fig. 9). The level of H_2O_2 starts increasing 6 h after infiltration and continues up to 24 h after infiltration. On other hand, the level of H_2O_2 remained at lower levels consistently in the control leaves. The macroscopic HR was also visible at the site of infiltration after 24 h. The *in vivo* H_2O_2 accumulation was also spotted as a brown precipitate using the DAB staining method in the harpin-treated tobacco leaves (Fig. 9a) whereas there was no such formation of brown precipitates in the control samples. All these results indicate accumulation of H_2O_2 in the harpin treated tobacco leaves. ROS generated by harpin was also evident and visualized in 6-, 12- and 24-hour post infiltration (hpi) while observed to be most prominent in 24 hpi leaf using a ROS-sensitive fluorescent dye 2',7'-dichlorodihydrofluorescein diacetate (DCFDA). This fluorescent dye detects broad range of ROS responses such as generation of H_2O_2 and superoxide anion O2-. The infiltrated purified harpin in tobacco leaves start the DCFDA reaction corresponding to a strong H_2O_2 burst as compared to buffer infiltrated leaves (control). The results from this DAB staining experiment showed that the fluorescence intensity of DCFDA increased in harpin treated leaf to a bigger extent as compared with buffer treated control leaves.

3.3.3 Quantification of Hydrogen peroxide using FOX reagent method

After infiltration of purified harpin, a rapid burst of ROS was observed by determining the levels of H_2O_2 at various time points. ROS was quantified in tobacco leaves using FOX reagent method and found that the first peak was visible at 6 hpi (7.55 μmol/FW) and then fluctuated till 12 hpi (10.03 μ mol/FW), the highest peak was observed at 24 hpi (11.85 μmol/FW) after that the level of H_2O_2 started declining at 48 hpi (5.55 μmol/FW) and at 72 hpi (2.75 μmol/FW) in harpin infiltrated leaves. However, the level of H_2O_2 was consistently lower in the leaves of control plants. All these results indicates that harpin can trigger the accumulation of H_2O_2 in *Nicotiana tabacum* leaves (Figure 9b).

3.3.4 Histological and cytological studies of harpin induced plant defense response

To clone, the harpin gene (*hrpZ2*, 1.03 kb) Localized plant cell death is a well-recognized defence response that restricts nutrient availability to the invading pathogens and limits their spread. To determine whether our harpin protein induces such localized cell death, tobacco leaves were infiltrated with the harpin and subsequently stained with trypan blue to visualize cell death (Fig. 10a). The results clearly showed that harpin treatment induced localized cell death or programmed cell death (PCD) at the site of infiltration and its surrounding area. This defense response is indicative of a hypersensitive reaction of plant to restrict the pathogen invasion and prevent systemic infection.

Callose is a polysaccharide that plays an important role in a variety of processes during the plant development and in defense responses. Callose deposition was determined by aniline blue staining of leaf samples followed by observation under confocal microscopy. The images of aniline blue staining of leaves after infiltration is shown in figure 10b. Quantitative assessment of the number of callose deposits per mm^2 leaf tissue is shown in figure 10b. The results show that there were different patterns of callose deposition depending on the time point that were being observed. While there was no callose deposition observed in the control leaves, the results suggested that harpin induced the callose deposition in harpin infiltrated leaves.

This is a provisional file, not the final typeset article

3.3.5 Analysis of plant defense related enzymes in response to harpin

Harpin also results in the elicitation of defense-related enzymes. The defense-related enzymes such as PAL and PPO were influenced in harpin infiltrated leaves. PPO activity was considerably increased in harpin treated leaves compared with control. Results show that the activity of PPO starts increasing 6 h after infiltration and continues up to 24 h after infiltration. The activity of PPO in harpin infiltrated leaves was higher than control leaves with maximum activity observed at 24 hpi (329.21 U/g), after which the level of activity started to decline at 48 and 72 hpi (Fig. 11a). Finally, we conclude that the activity of PPO in harpin treated leaves was higher compared to the control leaf samples.

Our results show another key enzyme, i.e., phenylalanine ammonia lyase (PAL), which plays an essential role in plant defense during plant microbes' interaction, was also regulated in response to harpin protein in tobacco leaves. At the beginning, the activity level of PAL showed moderate activity (21.12 U/g) upto 4 hpi. The maximum activity of PAL was recorded 24 h after infiltration (63.36 U/g) while it declined noticeably 48 h after infiltration (Fig. 11b). Finally, we concluded that the activity of PAL in harpin treated leaves was higher compared to the control.

After infiltration of purified harpin, the levels of H_2O_2 were examined at various time points and which resulted a rapid burst of ROS. ROS was quantified in tobacco leaves by FOX reagent method and found that the first peak was visible at 6 hpi (7.55 µmol/FW) and then fluctuated till 12 hpi (10.03 µ mol/FW). The highest peak was observed at 24 hpi (11.85 µmol/FW). After that, the level of H_2O_2 started declining at 48 hpi (5.55 µmol/FW) and 72 hpi (2.75 µmol/FW) in harpin infiltrated leaves. However, the level of H_2O_2 was consistently lower in the leaves of control plants. All these results indicate that after infiltration, harpin triggers an accumulation of H_2O_2 and ROS burst in *Nicotiana tabacum* leaves in a time-dependent manner (Figure 11).

4 Discussion

Plant responses to pathogenic attack are highly complex and entails a multitude of biochemical and cellular procedures. One of the key components of plant defense is the HR, a form of localized programmed cell death that serves to limit pathogen spread by restricting it to the initial site of infection (Balint-Kurti 2019). We identified a novel harpin elicitor from *Pseudomonas syringae*, which elicited a hypersensitive response in wide spectrum of non-host plants. The protein sequence analysis revealed that this harpin protein (HrpZ2) is different from the previous harpin ($HrpZ_{Pss}$) reported from *Pseudomonas syringae* pv. *syringae*. The total number of amino acid residues in HrpZ2 is 342, while that in $HrpZ_{Pss}$ is 341 (Fig 1). The major differences observed between these two proteins ($HrpZ_{Pss}$ *vs* HrpZ2) are listed in the Table 2.

In silico analysis of the physicochemical properties of harpin protein gave us many valuable insights into its biological properties. Harpin is structurally stable with an instability index of 35.97 (Table. 1) and thermally robust. Other characteristics such as hydropathy (GRAVY) and aliphatic index are in accordance with to its solubility as well as thermal properties. These characteristics make harpin suitable for the development of elicitor-based plant protection strategies. Based on the analysis of amino acid residues, the theoretical isoelectric point (pI) of the harpin was predicted to be 4.93 (Table. 1), suggesting that the protein is acidic and would carry a net negative charge under physiological conditions (pH = 7.0).

Analysis of the predicted secondary structure of harpin protein revealed a distinctive structural organization characterized by the presence of alpha helices (50.29 %), followed closely by random coils (48.53 %), with a minimal presence of beta sheets (1.16 %) (Figure 1). The high proportion of coil regions, comprising nearly half of the total protein structure, indicates a dynamic and flexible

architecture that may be essential for conformational adaptability during host-pathogen interactions. Further analysis of intrinsically disordered regions (IDRs) indicated that nearly 42 % (144 residues) of harpin protein lacks a stable tertiary structure (Figure 1). IDRs are recognized for their role in mediating protein-protein and protein-nucleic acid interaction, primarily where binding adaptability, rapid conformational deviations, and dynamic regulation are needed. These attributes are particularly relevant to harpin`s function as an effector protein, enabling it to interact flexibly with components of the plant defense machinery and effectively trigger immune responses.

Presence of IDRs and their functional importance is well documented both in prokaryotic and eukaryotic systems. Tardigrade, a microscopic eukaryotic animal, has intrinsically disordered proteins (IDPs) and is capable of surviving in extreme environmental circumstances (Boothby et al., 2017). These IDPs, including cytosolic abundant heat-soluble (CAHS) proteins, contribute to stress tolerance against desiccation and radiation in tardigrades (Yamaguchi et al., 2012). These proteins maintain amorphous, gel-like protective environments that stabilize macromolecules without demanding fixed conformations. Tardigrade IDPs work through structural plasticity, allowing transient, multivalent interactions critical for their survival under extreme stress conditions. Likewise, in prokaryotic systems, effector proteins with large IDR content have been reported. For example, effector YopM from *Yersinia* species and *E. coli*'s Tir contain extensive disordered regions that encourage host protein hijacking and modulation of the immune system (Marín et al., 2013). These effectors utilize intrinsically disordered regions (IDRs) to interact with targets flexibly. Therefore, the presence of large IDRs in harpin is not an exceptional feature; rather, it is a conserved evolutionary approach used by pathogens as well as extremophiles for adaptation, survival, and infection. Pertaining to plant-microbe interactions, these disordered regions of harpin may offer flexible interactions, adaptability, and the ability to promptly trigger plant immune signaling, which makes it a powerful elicitor of plant defense.

Since the initial identification of harpin from *Erwinia amylovora* by Wei et al. (1992), the harpin protein has been extensively studied for its role in eliciting HR and induction of plant immune response. Despite decades of research, the experimental determination of harpin`s crystal structure remains unresolved till date. This lack of structural information has posed a significant barrier in understanding the molecular mechanisms underlying its interaction with plant receptors as well as how it regulates immune responses. To address this knowledge gap, a three-dimensional (3D) model of harpin protein was predicted by our lab using computational modelling approaches (Fig. 2a). Structural validation was performed using Ramachandran plot and ProSA server, revealing that 99 % of residues fall in allowed as well as additionally allowed regions (indicating a well-refined model) (Fig. 2b). In contrast, only 0.7 % of residues are in disallowed regions. The Z-score of our computed 3D-model of harpin protein as assessed by the ProSA server is -5.03 (Fig. 2c), suggesting high stereochemical quality. The overall correctness and reliability of the predicted model support and indicate that the predicted model is reliable. In the absence experimentally resolved crystal structure, our *in silico* validated model provides a reliable framework for investigating the structural and functional properties of harpin, particularly its interactions with host immune components (Lal et al., 2023).

The phylogenetic analysis of 48 harpin proteins of different bacterial genera was done. It shows that harpins such as HrpZ1 from *P. syringae* pv. tomato and HrpZ2 from other *Pseudomonas* pathovars clustered together in a single clade, but with significant intra-genus diversity, suggesting possible functional divergence or adaptation to different plant hosts (Fig 6). The phylogenetic proximity of certain harpins across genera, such as between *Dickeya dadantii* and *Pectobacterium atrosepticum*, also reflects their close taxonomic relationship and possible conservation of pathogenicity mechanisms. The HrpN proteins derived from *Erwinia amylovora* pathovars clustered together in another well-supported, distinct clade (indicated in red). This suggests a conserved

This is a provisional file, not the final typeset article

evolutionary pathway that is separate from the harpins found in *Pseudomonas syringae* pathovars, such as HrpZ, HrpW, and HopP1.

The harpin (HrpZ2) protein was successfully purified from *E.coli* BL21 cells harbouring the harpin gene construct and the purity of the protein was assessed by running SDS PAGE (Figure 7), followed by the quantification of protein through Bradford Assay which was found to be 132 µg/ml. Defensive reactions to phytopathogens include multiple mechanisms, like the rapid production of ROS and the initiation of HR (Balint-Kurti 2019). We investigated H_2O_2 accumulation as a defense response triggered by harpin. In defense signalling pathways, ROS can act as a second messenger (Li et al., 2018). The stimulation of defense-related enzymes and increased resistance to infections are the results of exogenous application or overproduction of H_2O_2 and various prooxidants in plants (Mohammadi et al., 2021; Wang et al., 2020). Pathways that enhance cellular apoptosis can be activated by H_2O_2 (Mittler 2002). It has been demonstrated, therefore, that H_2O_2 does not function as a signal regulator for cell death or in the synthesis of phytoalexins in other systems (Mur et al., 2005). As per our DAB staining results, the harpin-induced H_2O_2 accumulation was concentrated in distinct regions that corresponded to harpin infiltration sites rather than being evenly distributed across the leaf surface. DAB staining in harpin treated plants developed a reddish-brown colour at the local infiltrated area (Figure 9). The results from time course experiments showed that, like DAB staining, the DCFDA fluorescence intensity increased at 24 hpi to a greater extent than in buffer treated plants (control). The infiltrated harpin initiated the DCFDA reactions in tobacco leaf tissues corresponding to a strong H_2O_2 burst in treated leaves compared with untreated leaves: peaked at 24 hpi, after treatment (Figure 9b). Upon quantification of harpin in tobacco leaves by FOX reagent method, it was observed that there was high amount of H_2O_2 corresponding to 9.86 µ mol / FW in harpin infiltrated leaves as compared with buffer infiltration (Figure 9). Cellular death resulting from HR at the infiltrated region halted the further dissemination of bacterial pathogens in living tissues. Trypan blue staining indicated HR cell death in the infiltrated leaves of the tobacco plants. The hypersensitive area developed a deep bluish colour upon trypan blue staining which was visualized after 3 dpi (Figure 10a). The substantial accumulation of H_2O_2 and HR cell death triggered by harpin infiltration contributed to the localized hypersensitive response. In the early stages of bacterial infections, callose deposition acts as a physical barrier (thickened cell wall) to help shield the cell from pathogens. Furthermore, H_2O_2 could promote callose deposition to fortify cell walls (Wu et al., 2018).

In our study, we reported that for leaves infiltrated with harpin, callose accumulation was higher than in the control (Figure 10b). As visualized under confocal microscope, tobacco leaves with a harpin-treated area of the sample at 24 hpi had many callose bright light blue dots, suggesting that harpin was functioning well in the plant system in mounting HR. There were no callose observations in the buffer-treated leaves of the plants, maximum callose accumulation occurred at 24 hpi as compared to buffer treated plants. To determine the enzymatic activities at 0- and 24-hpi, tobacco leaves infiltrated with harpin (30 µg/ml) were collected, and the activity of harpin was compared with that of buffer as a negative control. According to (Figure 11), harpin infiltration resulted in varied increases in PAL and PPO activity, which were substantially different from the controlled treatment. A significant enzyme linked to disease resistance is PPO, and a rise in PPO activity in leaves treated with harpin suggested that the plant had shown a high level of disease resistance. Following harpin application, the PPO activity in tobacco increased significantly at 24 hpi reaching the level of 23.3 U/FW. The activities of PPO in harpin-treated tobacco leaves were found to be higher than those in buffer infiltrated leaves during the entire experimental period (Figure 11A). The activity of PAL increased at 24 hpi reaching the level of 32U/FW following harpin infiltration (Figure 11B). According to the above-mentioned findings, harpin treatment increased the generation of two

protective enzymes (PAL and PPO) to increase plants' resistance to disease. Our findings are consistent with recent reports by (Li et al., 2011; Wang et al., 2011) that describe similarities in the induction of defense related enzymes from *Nicotiana tabacum* and *Pinellia ternata* respectively during exogenous application of PopW in *N. tabacum* and application of Hpa1. In *P. ternata*, their data showed that the same enzymes (PAL and PPO) in addition to peroxidase (POD) were upregulated to around 2.5-folds during both kinds of interactions, with differences in timing and extent. Moreover, our data of histochemical detection of harpin infiltration also correlates with these recent studies. Nevertheless, additional research is required to better understand the roles and associated mechanisms of the harpin-induced hypersensitive response signalling pathway in order to qualify it as a biological control agent for usage in agricultural settings.

In summary, further research is needed to comprehensively elucidate the temporal dynamics of H_2O_2 accumulation, defense related enzymes, callose deposition, and programmed cell death during plant-pathogen or elicitor triggered interactions. To conclude, a novel harpin (HrpZ2) from *Pseudomonas syringae*, induced hypersensitive response in *Nicotiana tabacum*, a non-host plant species, which is associated with various biochemical events such as H_2O_2 and ROS production, callose deposition and expression of various enzymes involved in defense responses. These findings highlight HrpZ2`s potential role as an effector in triggering immune responses and provide a foundation for further exploration in to its molecular interactions and mechanisms of action.

5 Conclusions

A recombinant HrpZ2 protein from *Pseudomonas syringae* was successfully expressed and purified, and it was found to be biological active as confirmed through HR induction assays in *Nicotiana tabacum*. The present study clearly showed that this novel harpin (HrpZ2) caused a significant increase in the activities of two key defense enzymes, PPO and PAL, in *Nicotiana tabacum*. Both enzymes showed a time-dependent increase, with notable peak activities at 24 hpi, coinciding with other defense responses such as hydrogen peroxide (H□O□) burst, HR cell death, and callose accumulation. The study also demonstrated that harpins can induce HR in a wide range of non-host plants. These findings highlight harpins' effectiveness in activating plant immune signaling pathways and underscore its potential role in induced resistance strategies for sustainable crop protection. The upregulation of PPO and PAL supports the idea that harpin acts as a powerful elicitor molecule capable of priming plants for improved resistance against pathogens. Due to the lack of an experimentally determined crystal structure, our validated *in silico* model provides a crucial foundation for future functional assays and interaction studies using plant receptor proteins or synthetic analogs.

6 Conflict of Interest

The authors declare that the research was conducted in the absence of any commercial or financial relationships that could be construed as a potential conflict of interest.

7 Author Contributions

KL: Methodology, Investigation, Formal analysis, Visualization, Writing– original draft. AJ: Investigation, Writing – review & editing. VS: Investigation, Writing –review & editing. MM: Data Analysis, Writing– review & editing. PS: Data Analysis, Writing – review & editing. DD: Conceptualization, Investigation, Formal analysis, Visualization, Funding acquisition, Project administration, Resources, Supervision, Writing - original draft, Writing–review & editing.

This is a provisional file, not the final typeset article

8 Funding

DD and Laboratory of Plant Biotechnology gratefully acknowledges the financial support provided by various funding agencies. This includes UGC-BSR-Startup Research Grant (F.30-544/2021(BSR)) from UGC, Govt. of India (GoI); and the Seed grant (R/Dev/D/IoE/Equipment/Seed Grant/2021-22/42404) awarded to DD under the Institute of Eminence (IoE) scheme by Banaras Hindu University (BHU), Varanasi. Financial assistance from the Department of Biotechnology (DBT), Govt. of India, to the School of Biotechnology, BHU, is also duly acknowledged. The authors further acknowledge the support provided in the form of DBT-Senior Research Fellowship (SRF) to KL and the Postgraduate stipend to AJ from the DBT, Government of India.

9 Data Availability Statement

The original contributions presented in the study are included in the article/supplementary material. Further inquiries can be directed to the corresponding author.

10 References

1. Balint-Kurti, P. (2019). The plant hypersensitive response: concepts, control and consequences. *Mol. Plant Pathol.* 20, 1163-1178. doi: 10.1111/mpp.12821
2. Bi, Y. M., Kenton, P., Mur, L., Darby, R., and Draper, J. (1995). Hydrogen peroxide does not function downstream of salicylic acid in the induction of PR protein expression. *Plant J.* 8, 235-245. doi: 10.1046/j.1365-313x.1995.08020235.x
3. Bogdanove, A. J., Beer, S. V., Bonas, U., Boucher, C. A., Collmer, A., Coplin, D. L., et al. (1996). Unified nomenclature for broadly conserved *hrp* genes of phytopathogenic bacteria. *Mol. Microbiol* 20, 681-683. doi: 10.1046/j.1365-2958.1996.5731077.x
4. Boothby, T. C., Tapia, H., Brozena, A. H., Piszkiewicz, S., Smith, A. E., Giovannini, I., et al. (2017). Tardigrades use intrinsically disordered proteins to survive desiccation. *Mol. Cell*, 65, 975-984. doi: 10.1016/j.molcel.2017.02.018
5. Bowie, J. U., Lüthy, R., and Eisenberg, D. (1991). A method to identify protein sequences that fold into a known three-dimensional structure. *Science* 253, 164-170. doi: 10.1126/science.1853201
6. Bradford, M. M. (1976). A rapid and sensitive method for the quantitation of microgram quantities of protein utilizing the principle of protein-dye binding. *Anal. Biochem.* 72, 248-254. doi: 10.1016/0003-2697(76)90527-3
7. Chen, C. T., Yang, C. Y., and Tzen, J. T. C. (2022). Molecular characterization of polyphenol oxidase between small and large leaf tea cultivars. *Sci. Res.* 12, 14026. doi: 10.1038/s41598-022-17184-1
8. Cheng, G. W., and Breen, P. J. (1991). Activity of phenylalanine ammonia-lyase (PAL) and concentrations of anthocyanins and phenolics in developing strawberry fruit. *J. Amer. Soc. Hort. Sci.* 116, 865-869. doi: 10.21273/JASHS.116.5.865
9. Cho, H. J., Park, Y. J., Noh, T. H., Kim, Y. T., Kim, J. G., Song, E. S., et al. (2008). Molecular analysis of the *hrp* gene cluster in *Xanthomonas oryzae* pathovar *oryzae* KACC10859. *Microb. Pathog.* 44, 473-483. doi: 10.1016/j.micpath.2007.12.002
10. Choi, M. S., Heu, S., Paek, N. C., Koh, H. J., Lee, J. S., and Oh, C. S. (2012). Expression of *hpa1* gene encoding a bacterial harpin protein in *Xanthomonas oryzae* pv. *oryzae* enhances

disease resistance to both fungal and bacterial pathogens in rice and *Arabidopsis*. *Plant Pathol. J.* 28, 364-372. doi: 10.5423/PPJ.OA.09.2012.0136

11. Choi, M. S., Kim, W., Lee, C., and Oh, C. S. (2013). Harpins, multifunctional proteins secreted by gram-negative plant-pathogenic bacteria. *Mol. Plant-Microbe Interact.* 26, 1115-1122. doi: 10.1094/MPMI-02-13-0050-CR
12. Chuang, H. W., Harnrak, A., Chen, Y. C., and Hsu, C. M. (2010). A harpin-induced ethylene-responsive factor regulates plant growth and responses to biotic and abiotic stresses. *Biochem. Biophys. Res. Commun.* 402, 414-420. doi: 10.1016/j.bbrc.2010.10.047.
13. Collmer, A., and Beer, S. V. (1998). "5.3 *hrp* Genes and their function". in Methods in Microbiology, ed. P. Williams, J. Ketley, and G. Salmond, (Academic Press), Volume 27, 139-148. doi: 10.1016/S0580-9517(08)70277-0
14. Colovos, C., and Yeates, T. O. (1993). Verification of protein structures: patterns of nonbonded atomic interactions. *Prot. Sci.* 2, 1511-1519. doi: 10.1002/pro.5560020916
15. Cozzetto, D., Minneci, F., Currant, H., and Jones, D. T. (2016). FFPred 3: feature-based function prediction for all Gene Ontology domains. *Sci. Rep.* 6, 31865. doi: 10.1038/srep31865
16. Cui, H., Tsuda, K., and Parker, J. E. (2015). Effector-triggered immunity: from pathogen perception to robust defense. *Ann. Rev. Plant Biol.* 66, 487-511. doi: 10.1146/annurev-arplant-050213-040012
17. Daudi, A., and O'Brien, J. A. (2012). Detection of Hydrogen Peroxide by DAB Staining in Arabidopsis Leaves. *Bio-protocol* 2, e263.
18. Dodds, P. N., and Rathjen, J. P. (2010). Plant immunity: towards an integrated view of plant-pathogen interactions. *Nature Rev. Genet.* 11, 539-548. doi: 10.1038/nrg2812
19. Dong, H. P., Yu, H., Bao, Z., Guo, X., Peng, J., Yao, Z., et al. (2005). The ABI2-dependent abscisic acid signalling controls HrpN-induced drought tolerance in *Arabidopsis*. *Planta* 221, 313-327. doi: 10.1007/s00425-004-1444-x
20. Faris, J. D., Zhang, Z., Lu, H., Lu, S., Reddy, L., Cloutier, S., et al. (2010). A unique wheat disease resistance-like gene governs effector-triggered susceptibility to necrotrophic pathogens. *Proc. Natl. Acad. Sci. U. S. A.* 107, 13544-13549. doi: 10.1073/pnas.1004090107
21. Ferrer, J. L., Austin, M. B., Stewart, C., Jr, and Noel, J. P. (2008). Structure and function of enzymes involved in the biosynthesis of phenylpropanoids. *Plant Physiol. Biochem.* 46, 356-370. doi: 10.1016/j.plaphy.2007.12.009
22. Gasteiger, E., Hoogland, C., Gattiker, A., Duvaud, S., Wilkins, M.R., Appel, R.D. et al. (2005). "Protein identification and analysis tools on the ExPASy server" in The Proteomics protocols handbook, ed. J.M. Walker, (Humana Press, New York), 571-607. doi: 10.1385/1-59259-890-0:571
23. Haghpanah, M., Namdari, A., Kaleji, M. K., Nikbakht-Dehkordi, A., Arzani, A., and Araniti, F. (2025). Interplay between ROS and hormones in plant defense against pathogens. *Plants* 14, 1297. doi: 10.3390/plants14091297
24. He, S. Y., Huang, H. C., and Collmer, A. (1993). *Pseudomonas syringae* pv. *syringae* harpin$_{Pss}$: a protein that is secreted *via* the Hrp pathway and elicits the hypersensitive response in plants. *Cell* 73, 1255–1266. doi: 10.1016/0092-8674(93)90354-s
25. Hueck, C. J. (1998). Type III protein secretion systems in bacterial pathogens of animals and plants. *Microbiol. Mol. Biol. Rev.* 62, 379-433. doi: 10.1128/mmbr.62.2.379-433.1998

This is a provisional file, not the final typeset article

26. Ishida, T., and Kinoshita, K. (2007). PrDOS: prediction of disordered protein regions from amino acid sequence. *Nucleic Acids Res.* 35, W460-W464. doi: 10.1093/nar/gkm363
27. Jiang, Z. Y., Woollard, A. C., and Wolff, S. P. (1990). Hydrogen peroxide production during experimental protein glycation. *FEBS Lett.* 268, 69-71. doi: 10.1016/0014-5793(90)80974-n
28. Jones, D. T. (1999). Protein secondary structure prediction based on position-specific scoring matrices. *J. Mol. Biol.* 292, 195-202. doi: 10.1006/jmbi.1999.3091
29. Jones, J. D., & Dangl, J. L. (2006). The plant immune system. *Nature* 444, 323-329. doi: 10.1038/nature05286
30. Galán, J. E., and Collmer, A. (1999). Type III secretion machines: bacterial devices for protein delivery into host cells. *Science* 284, 1322-1328. doi: 10.1126/science.284.5418.1322
31. Koch, E., and Slusarenko, A. (1990). *Arabidopsis* is susceptible to infection by a downy mildew fungus. *Plant Cell* 2, 437-445. doi: 10.1105/tpc.2.5.437
32. Lal, K., Singh, V. K., and Dey, D. (2023). Study of molecular interaction between *Arabidopsis* aquaporin and *Pseudomonas syringae* pv. *syringae* harpin ($HrpZ_{Pss}$) through molecular docking tools. *Int. J. Plant Env.* 9, 343-349. doi: 10.18811/ijpen.v9i04.06
33. Laskowski, R. A., Rullmannn, J. A., MacArthur, M. W., Kaptein, R., and Thornton, J. M. (1996). AQUA and PROCHECK-NMR: programs for checking the quality of protein structures solved by NMR. *J. Biomol. NMR* 8, 477–486. doi: 10.1007/BF00228148
34. Lavanya, S. N., Niranjan-Raj, S., Jadimurthy, R., Sudarsan, S., Srivastava, R., Tarasatyavati, C., et al. (2022). Immunity elicitors for induced resistance against the downy mildew pathogen in pearl millet. *Sci. Rep.* 12, 4078. doi: 10.1038/s41598-022-07839-4
35. Letunic, I., and Bork, P. (2024). Interactive Tree of Life (iTOL) v6: recent updates to the phylogenetic tree display and annotation tool. *Nucleic Acids Res.* 52, W78–W82. doi: 10.1093/nar/gkae268
36. Li, H., Luo, Y. F., Wang, Y. S., Yang, Q., Xiao, Y. L., Cai, H. R., et al. (2018). Using ROS as a second messenger, NADPH oxidase 2 mediates macrophage senescence *via* interaction with NF-κB during *Pseudomonas aeruginosa* infection. *Oxid. Med. Cell. Longev.* 2018, 9741838. doi: 10.1155/2018/9741838
37. Li, J. G., Cao, J., Sun, F. F., Niu, D. D., Yan, F., Liu, H. X., et al. (2011). Control of Tobacco mosaic virus by PopW as a result of induced resistance in tobacco under greenhouse and field conditions. *Phytopathol.* 101, 1202–1208. doi: 10.1094/PHYTO-02-11-0049
38. Li, L., Wang, H., Gago, J., Cui, H., Qian, Z., Kodama, N., Ji, H., Tian, S., Shen, D., Chen, Y., Sun, F., Xia, Z., Ye, Q., Sun, W., Flexas, J., & Dong, H. (2015). Harpin Hpa1 Interacts with Aquaporin PIP1;4 to Promote the Substrate Transport and Photosynthesis in Arabidopsis. *Scientific reports*, *5*, 17207. https://doi.org/10.1038/srep17207
39. Li, S. M., Hua, G. G., Liu, H. X., & Guo, J. H. (2008). Analysis of defence enzymes induced by antagonistic bacterium *Bacillus subtilis* strain AR12 towards *Ralstonia solanacearum* in tomato. *Annals Microbiol.* 58, 573-578. doi: 10.1007/BF03175560
40. Liu, Y., Zhou, X., Liu, W., Huang, J., Liu, Q., Sun, J. et al. (2020). HpaXpm, a novel harpin of *Xanthomonas phaseoli* pv. *manihotis*, acts as an elicitor with high thermal stability, reduces disease, and promotes plant growth. *BMC Microbiol* 20, 4. doi: 10.1186/s12866-019-1691-4
41. Luna, E., Pastor, V., Robert, J., Flors, V., Mauch-Mani, B., and Ton, J. (2011). Callose deposition: a multifaceted plant defense response. *Mol. Plant-Microbe Interact.* 24, 183–193. doi: 10.1094/MPMI-07-10-0149

42. Mandal, S., Kar, I., Mukherjee, A. K., and Acharya, P. (2013). Elicitor-induced defense responses in *Solanum lycopersicum* against *Ralstonia solanacearum*. *Sci. World J.* 2013, 561056. doi: 10.1155/2013/561056
43. Marín, M., Uversky, V. N., and Ott, T. (2013). Intrinsic disorder in pathogen effectors: protein flexibility as an evolutionary hallmark in a molecular arms race. *Plant Cell* 25, 3153–3157. doi: 10.1105/tpc.113.116319
44. Miao, X. Y., Qu, H. P., Han, Y. L., He, C. F., Qiu, D. W., and Cheng, Z. W. (2019). The protein elicitor Hrip1 enhances resistance to insects and early bolting and flowering in *Arabidopsis thaliana*. *PloS One* 14, e0216082. doi: 10.1371/journal.pone.0216082.
45. Mittler R. (2002). Oxidative stress, antioxidants and stress tolerance. *Trends Plant Sci* 7, 405-410. doi: 10.1016/s1360-1385(02)02312-9
46. Mohammadi, M. A., Cheng, Y., Aslam, M., Jakada, B. H., Wai, M. H., Ye, K., et al. (2021). ROS and oxidative response systems in plants under biotic and abiotic stresses: revisiting the crucial role of phosphite triggered plants defense response. *Front. Microbiol.* 12, 631318. doi: 10.3389/fmicb.2021.631318
47. Moreno, J., Nielsen, H., Winther, O., and Teufel, F. (2024). Predicting the subcellular location of prokaryotic proteins with DeepLocPro. *Bioinformatics* 40, btae677. doi: 10.1093/bioinformatics/btae677
48. Mur, L. A., Kenton, P., and Draper, J. (2005). In planta measurements of oxidative bursts elicited by avirulent and virulent bacterial pathogens suggests that H2O2 is insufficient to elicit cell death in tobacco. *Plant Cell Env.* 28, 548-561. doi: 10.1111/j.1365-3040.2005.01301.x
49. Nugent, T., and Jones, D. T. (2009). Transmembrane protein topology prediction using support vector machines. *BMC Bioinformatics*, 10, 1-11. doi: 10.1186/1471-2105-10-159
50. Nugent, T., Ward, S., and Jones, D. T. (2011). The MEMPACK alpha-helical transmembrane protein structure prediction server. *Bioinformatics* 27, 1438-1439. doi: 10.1093/bioinformatics/btr096
51. Pavli, O. I., Kelaidi, G. I., Tampakaki, A. P., and Skaracis, G. N. (2011). The *hrpZ* gene of *Pseudomonas syringae* pv. *phaseolicola* enhances resistance to rhizomania disease in transgenic *Nicotiana benthamiana* and sugar beet. *PloS One* 6, e17306. doi: 10.1371/journal.pone.0017306
52. Ricci, P. (1997). “Induction of the hypersensitive response and systemic acquired resistance by fungal proteins: the case of elicitins” in: Plant-Microbe Interactions, ed. G. Stacey, N.T. Keen, (Springer, Boston), 53-75. doi: 10.1007/978-1-4615-6019-7_3.
53. Tarafdar, P. K., Vedantam, L. V., Kondreddy, A., Podile, A. R., and Swamy, M. J. (2009). Biophysical investigations on the aggregation and thermal unfolding of harpin(Pss) and identification of leucine-zipper-like motifs in harpins. *Biochim. Biophys. Acta* 1794, 1684–1692. doi: 10.1016/j.bbapap.2009.07.023
54. Voigt C. A. (2014). Callose-mediated resistance to pathogenic intruders in plant defense-related papillae. *Front. Plant Sci.* 5, 168. doi: 10.3389/fpls.2014.00168
55. Wang, D., Wang, B., Wang, J., Wang, S., Wang, W., and Niu, Y. (2020). Exogenous application of harpin protein Hpa1 onto *Pinellia ternata* induces systemic resistance against tobacco mosaic virus. *Phytopathol.* 110, 1189–1198. doi: 10.1094/PHYTO-12-19-0463-R
56. Wei, W., Plovanich-Jones, A., Deng, W. L., Jin, Q. L., Collmer, A., Huang, H. C., et al. (2000). The gene coding for the Hrp pilus structural protein is required for type III secretion

This is a provisional file, not the final typeset article

of Hrp and Avr proteins in *Pseudomonas syringae* pv. *tomato*. *Proc. Natl. Acad. Sci. U. S. A.* 97, 2247–2252. doi: 10.1073/pnas.040570097.

57. Wei, Z. M., Laby, R. J., Zumoff, C. H., Bauer, D. W., He, S. Y., Collmer, A., et al. (1992). Harpin, elicitor of the hypersensitive response produced by the plant pathogen *Erwinia amylovora*. *Science* 257, 85–88. doi: 10.1126/science.1621099.
58. Wu, S. W., Kumar, R., Iswanto, A. B. B., and Kim, J. Y. (2018). Callose balancing at plasmodesmata. *J. Exp. Bot.* 69, 5325–5339. doi: 10.1093/jxb/ery317
59. Yamaguchi, A., Tanaka, S., Yamaguchi, S., Kuwahara, H., Takamura, C., Imajoh-Ohmi, S., et al. (2012). Two novel heat-soluble protein families abundantly expressed in an anhydrobiotic tardigrade. *PloS One*, 7, e44209. doi: 10.1371/journal.pone.0044209
60. Yarullina, L., Cherepanova, E. A., Burkhanova, G. F., Sorokan, A. V., Zaikina, E. A., Tsvetkov, V. O., et al. (2023). Stimulation of the defense mechanisms of potatoes to a late blight causative agent when treated with *Bacillus subtilis* bacteria and chitosan composites with hydroxycinnamic acids. *Microorganisms* 11, 1993. doi: 10.3390/microorganisms11081993
61. Zheng, W., Wuyun, Q., Li, Y., Liu, Q., Zhou, X., Peng, C., et al. (2025). Deep-learning-based single-domain and multidomain protein structure prediction with DI-TASSER. *Nature Biotechnology* 1-13. doi: 10.1038/s41587-025-02654-4
62. Zhu, F., Cao, M. Y., Zhang, Q. P., Mohan, R., Schar, J., Mitchell, M., et al. (2024). Join the green team: inducers of plant immunity in the plant disease sustainable control toolbox. *J. Adv. Res.* 57, 15-42. doi: 10.1016/j.jare.2023.04.016
63. Zipfel, C., Kunze, G., Chinchilla, D., Caniard, A., Jones, J. D., Boller, T., et al. (2006). Perception of the bacterial PAMP EF-Tu by the receptor EFR restricts *Agrobacterium*-mediated transformation. *Cell* 125, 749-760. doi: 10.1016/j.cell.2006.03.037

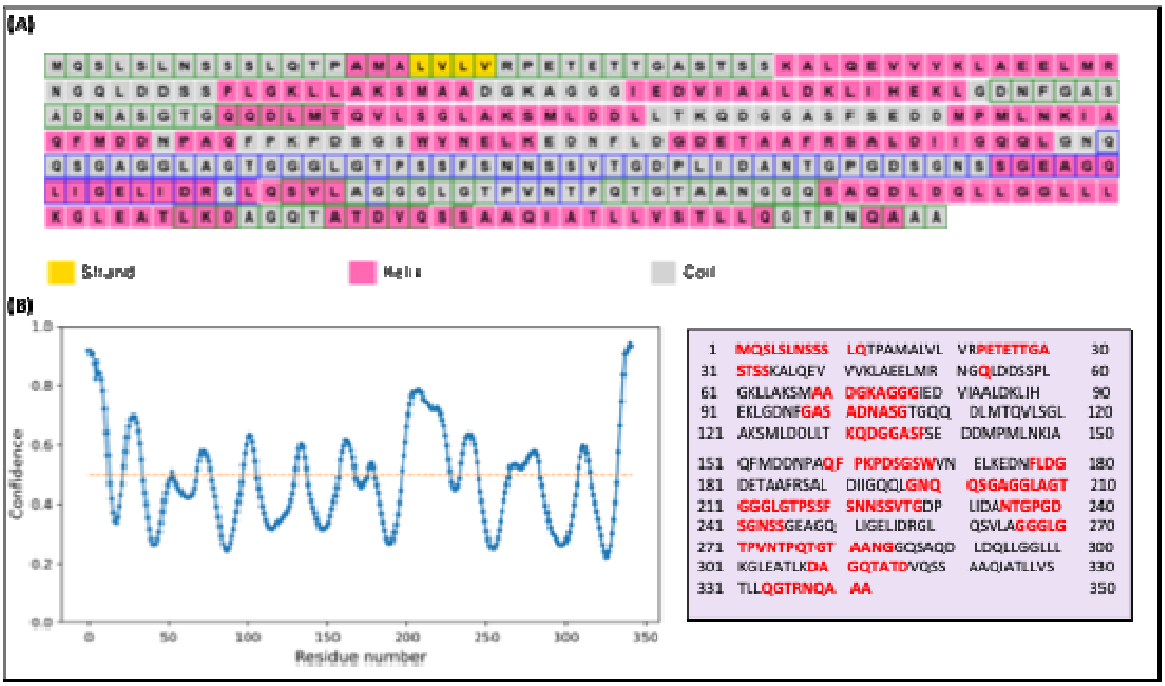

Fig. 1: Graphic representation of harpin secondary structure and intrinsic disordered regions. A) harpin was predicted to be composed of 50.29% (172 residues) alpha-helices, 48.53% (166 residues) random coils and only 1.16 % (4 residues) of beta sheets. B) left: graphical visualization of amino acid residues with the threshold of disordered score indicated by the yellow dotted line. PrDOS server predicted that 42% of harpin were of intrinsically disordered regions. Right side shows the total amino acid residues and the residues crossing the threshold of disorderliness are highlighted with red color.

This is a provisional file, not the final typeset article

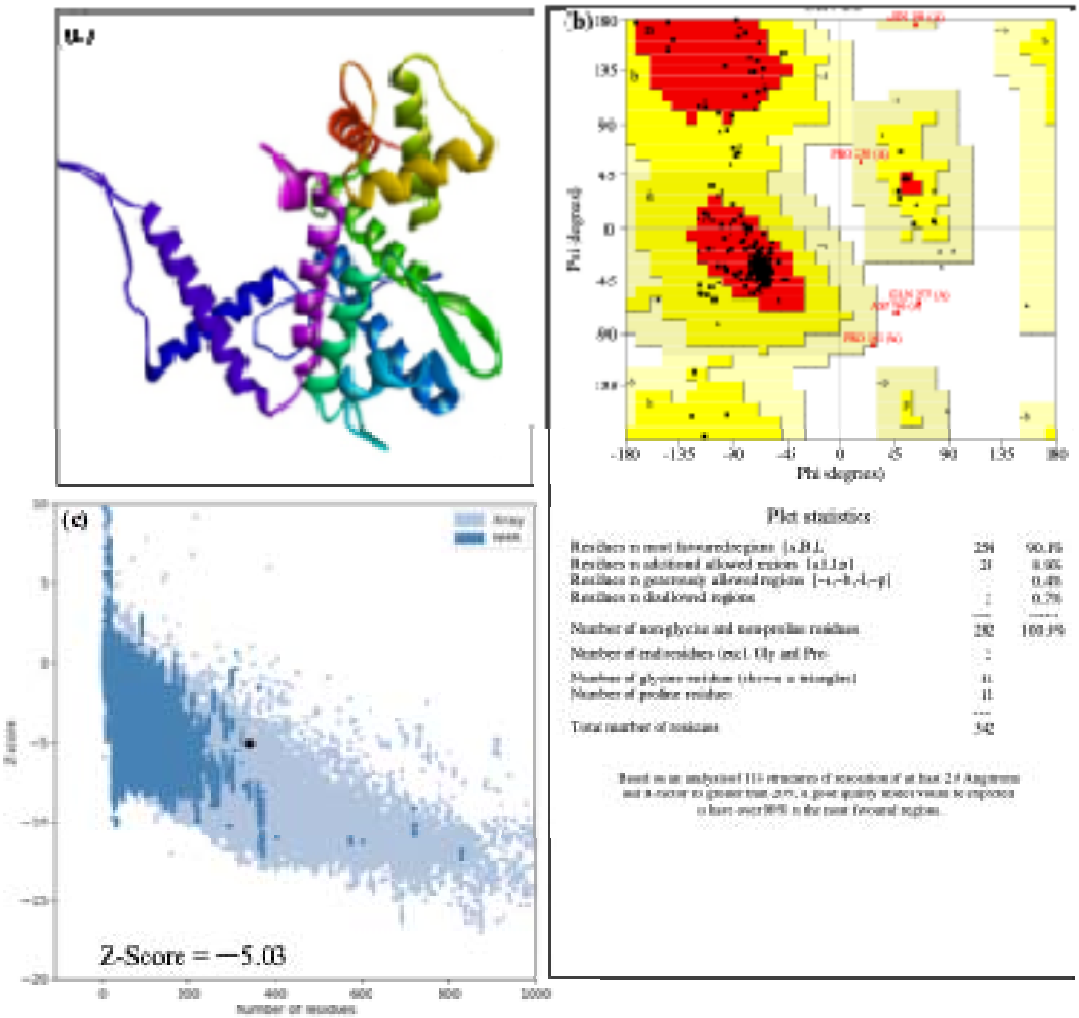

Fig. 2. *Ab-initio* model of harpin from *Pseudomonas syringae*. A) Ramachandran Plot validating the tertiary structure, (b) Statistical analysis of Ramachandran Plot of 3D structure of harpin. (b) 3D structure of harpin.

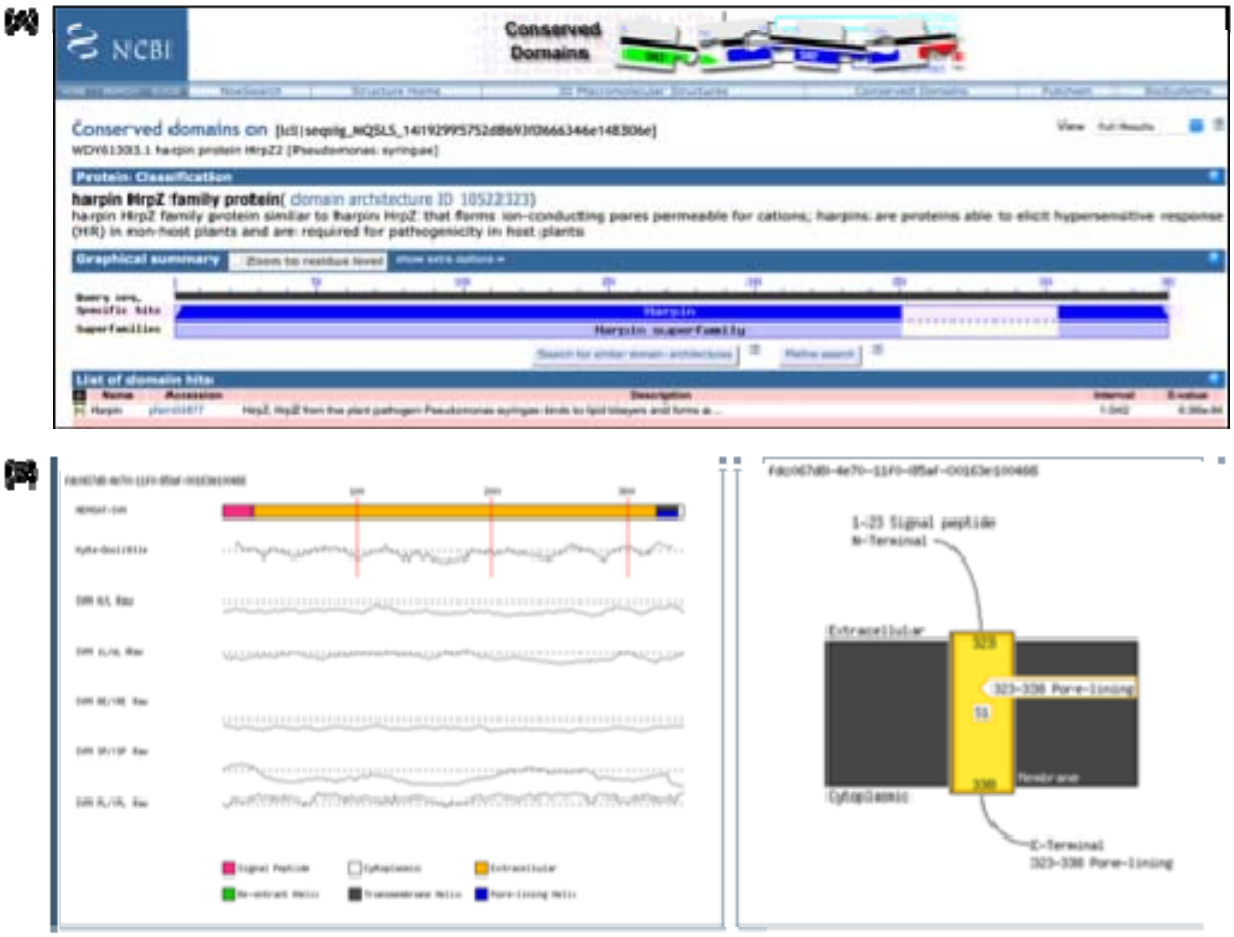

Fig. 3: Conserved domain analysis of harpin protein and its representative topology. A) Dark blue color shows the specific hits against the query sequences whereas light blue color shows the domain homology specifically to harpin protein. The representative diagram showing the topology of harpin protein detected by using the MEMSAT-SVM algorithm of PSIPRED webserver. **B)** left panel shows transmembrane regions (different color coded). Just below the transmembrane regions, the Kyte-Doolittle hydropathy plot followed by the four RAW outputs in trace forms (H/L & iL/oL: helix prediction PL: Pore lining residue, RE: Re-entrant helix residue, and SP: Signal peptide residue) used to predict the different regions in transmembrane are shown. **B)** Right panel shows the summarized cartoon of transmembrane helix topology showing the position of intra- and extracellular regions of protein.

This is a provisional file, not the final typeset article

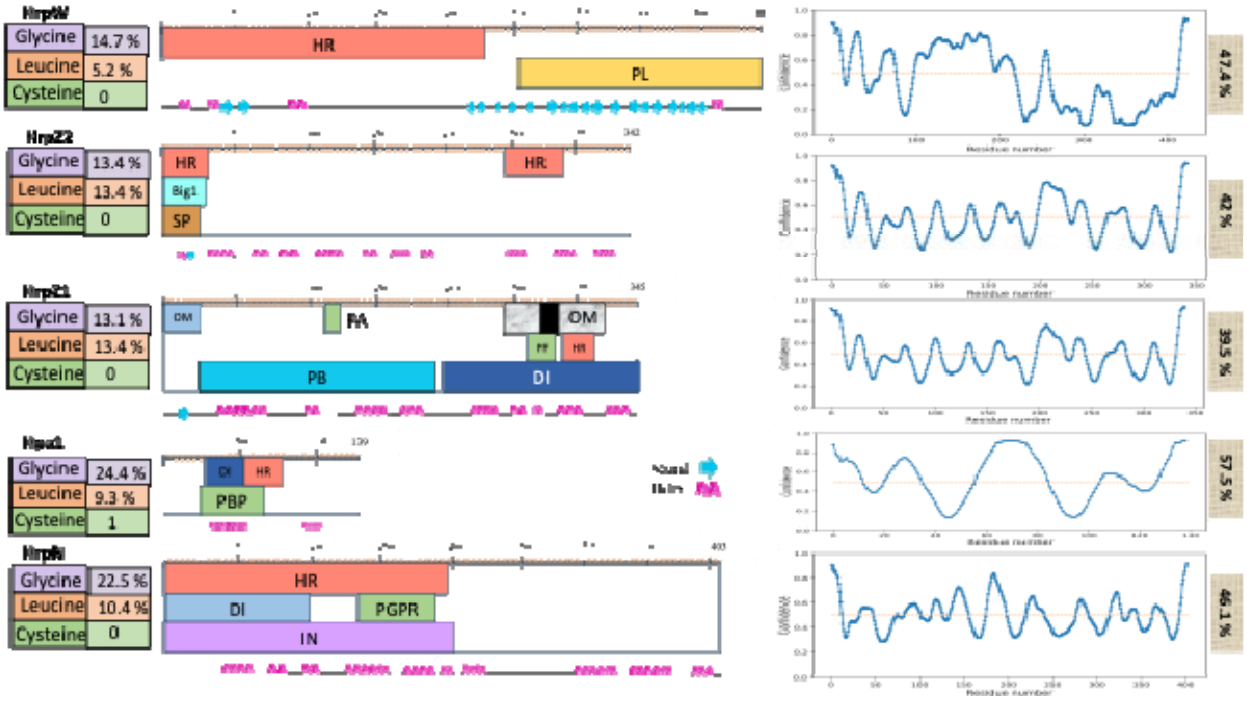

925

926 **Fig. 4:** Structural representation of functional domains of harpins from gram negative
927 phytopathogens: HrpN and HrpW (*Erwinia amylovora*); HrpZ1 and Hrp2 (*Pseudomonas syringae*),
928 and Hpa1 (*Xanthomonas oryzae*). PSIPRED prediction server was used to predict the secondary
929 structures of each harpin (showed at the bottom of each protein). The designated functional domains
930 were represented inside the protein. Each domain abbreviated in this figure are HR (hypersensitive
931 response), PL (pectate lyase), IN (interaction with a host protein), OM (oligomerization), PGP (plant
932 growth promotion), DI (defense induction), PA (phosphatidic acid binding), PF (pore formation), PB
933 (peptide binding). Glycine, leucine and cysteine richness are shown in left side while intrinsically
934 disordered regions (IDRs) of harpins are shown at the right side.

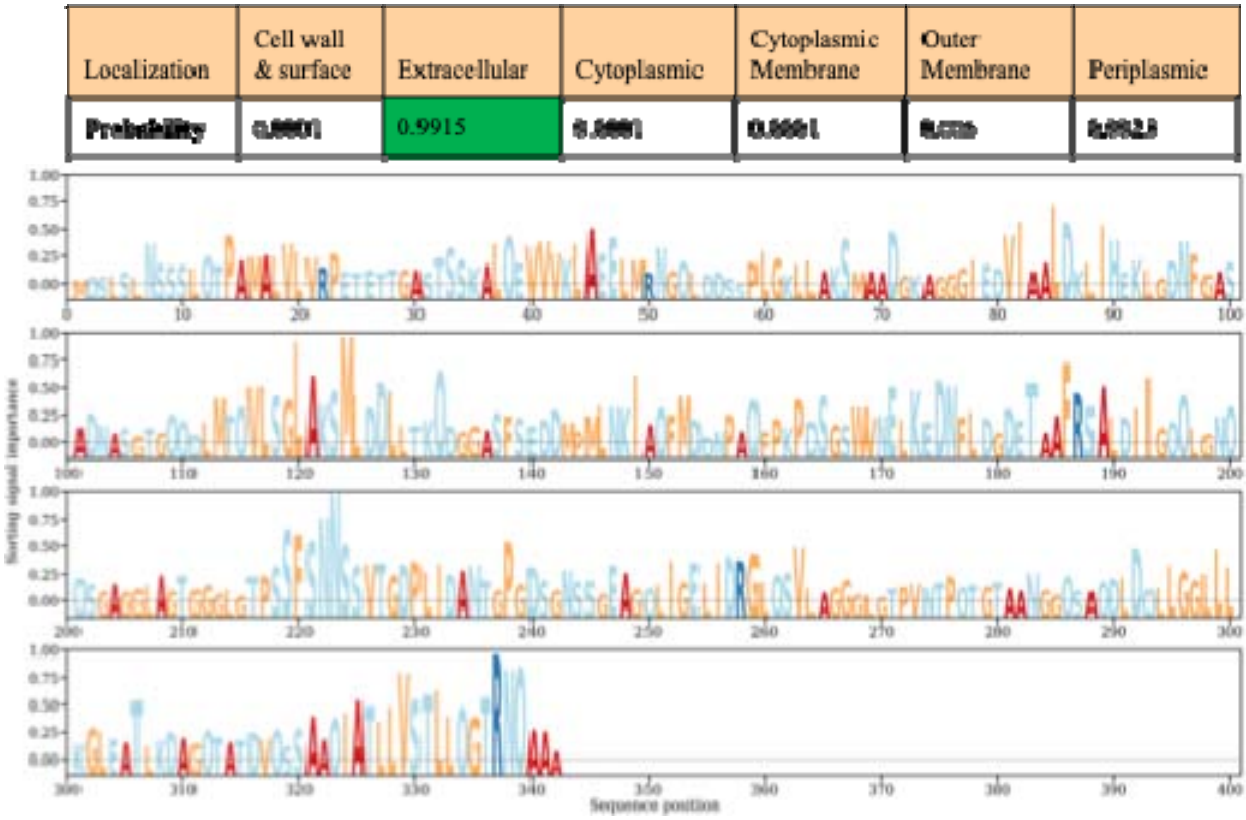

Fig. 5: The subcellular localization of harpin, as predicted by DeepLocPro-1.0, is graphically displayed in the image. At the top, a table shows that the harpin was predicted to have a subcellular localization with the highest probability of 0.9915 to the extracellular environment, which is highlighted in green. The lower portion of the image presents a graphical representation of the importance of sorting signals in relation to each amino acid residue targeted for cellular localization.

This is a provisional file, not the final typeset article

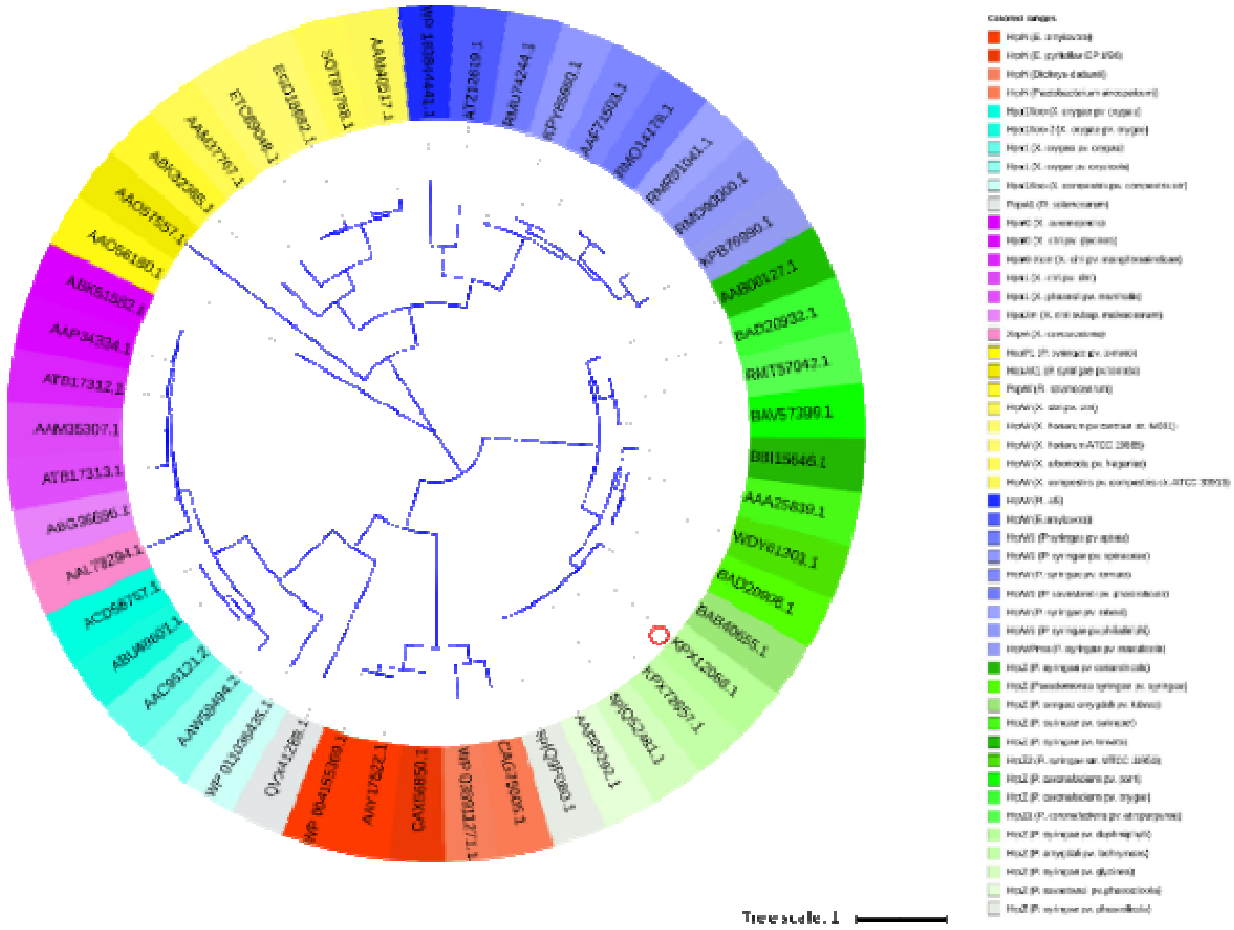

Fig. 6: Phylogenetic tree based on amino acid sequences from 48 different harpins from different genera was constructed using MEGA11.0 software. Each harpin is coded with a different color, and the representative names of all the accessories are given on the right side of the figure. The phylogenetic tree was visualized using the iTOL online tool (https://itol.embl.de/shared/2PuqbCYlUfiSH).

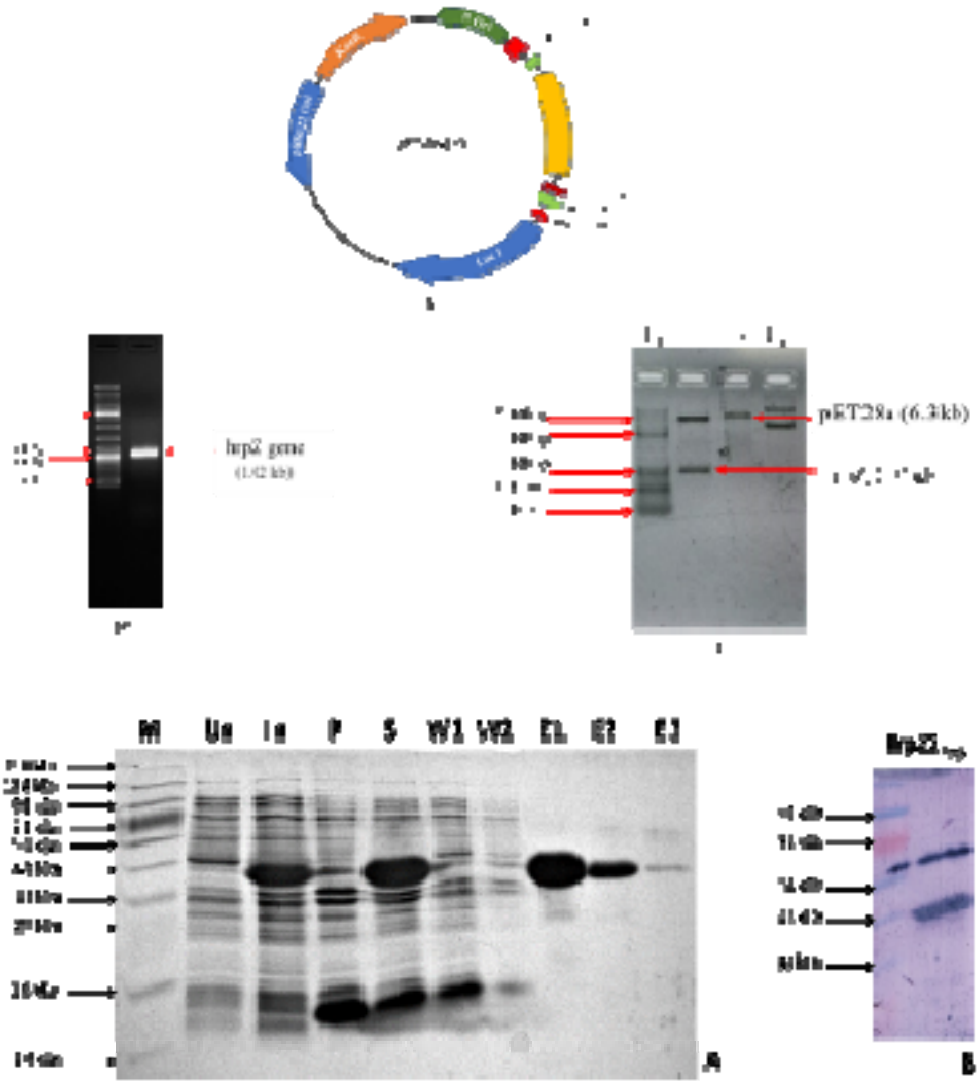

Fig. 7: Amplification of harpin gene (*hrpZ2*) and recombinant vector preparation. A). Recombinant vector *pET28a-hrpZ2* was prepared by double digestion of empty *pET28a* vector with *Nde*I and *Xho*I restriction enzymes and the double digested *hrpZ2* gene was cloned in digested empty *pET28a* vector to form a recombinant vector. Recombinant vector (*pET28a-hrpZ2*) was transformed into DH5α competent cells. The clone was confirmed by single and double digestion with *Xho*I, *Nde*I-*Xho*I restriction enzymes respectively. B) PCR amplification of harpin gene (*hrpZ2*) from the genomic DNA of *P. syringae*. L1 = Lane 1 showing molecular weight DNA ladder and L2 = lane 2 showing harpin gene (*hrpZ2*) amplification. C) Single and double digestion of the recombinant *pET28a-hrpZ2* construct, L1 = Lane 1 showing molecular weight DNA ladder and L2 = lane 2 showing double digested recombinant *pET28a-hrpZ2* vector (upper band) and releasing the harpin gene (*hrpZ2*) as insert (lowe band, 1.03 kb), lane 3 showing single digested recombinant *pET28a-hrpZ2* construct (~6.3 kb), lane 4 showing undigested empty *pET28a* vector.

This is a provisional file, not the final typeset article

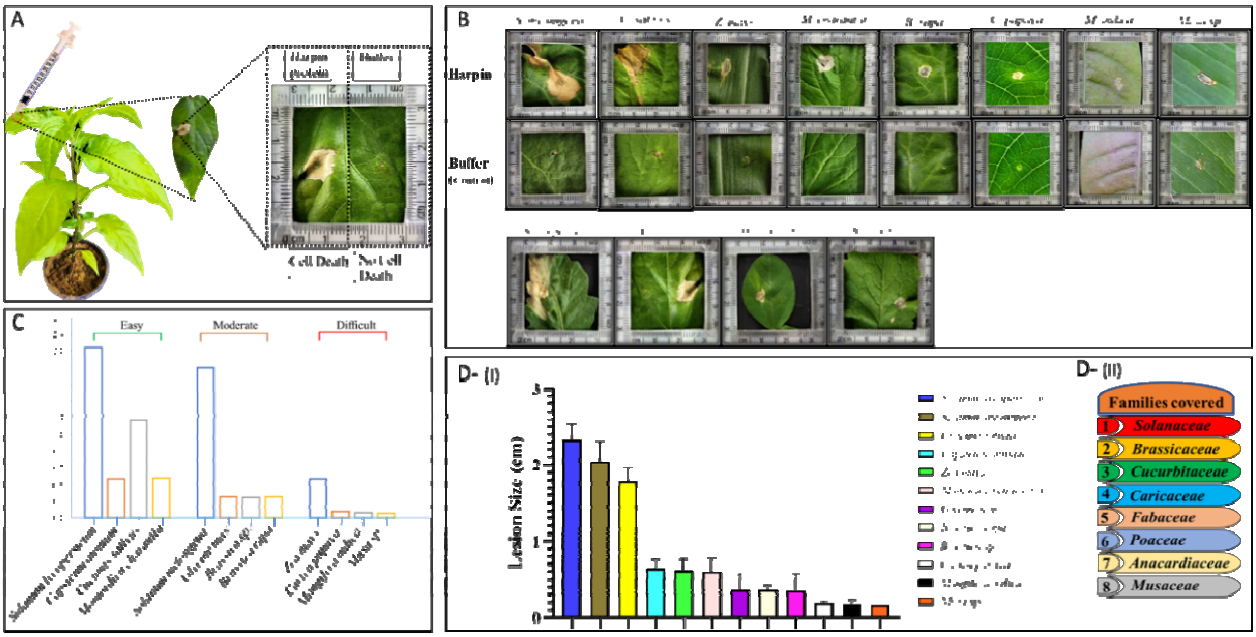

Fig. 8: Development of macroscopic HR on leaves of different non-host plants upon harpin infiltration. A, B) The purified harpin (50 ug/mL) was infiltrated at the abaxial surface of the leaves of non-host plants using 1 ml needless insulin syringe. The sodium phosphate buffer (10 mM), pH=7.5 was used as control. The photographs were taken at 3 dpi. C) Categorization of plants based on infiltration process. All the twelve plants where the infiltration was done and the hypersensitive response got generated were categorized into three groups: 1) easy, 2) moderate, 3) difficult. D(i)) Bar diagram of infiltration response obtained after infiltration in leaves of plants from eight different angiosperm families across the domain. Solanaceae (*Solanum lycopersicum*, *Capsicum annuum* and *Solanum melongena*), Brassicaceae (*Brassica rapa* and *Brassica* sp.), Cucurbitaceae (*Cucumis sativus* and *Momordica charantia*), Caricaceae (*Carica papaya*), Fabaceae (*Glycine max*), Poaceae (*Zea mays*), Anacardiaceae (*Mangifera indica*) and Musaceae (*Musa* sp.). D(ii)) Plant families covered to study the range of non-host plants responding with a HR response upon elicitation with harpin.

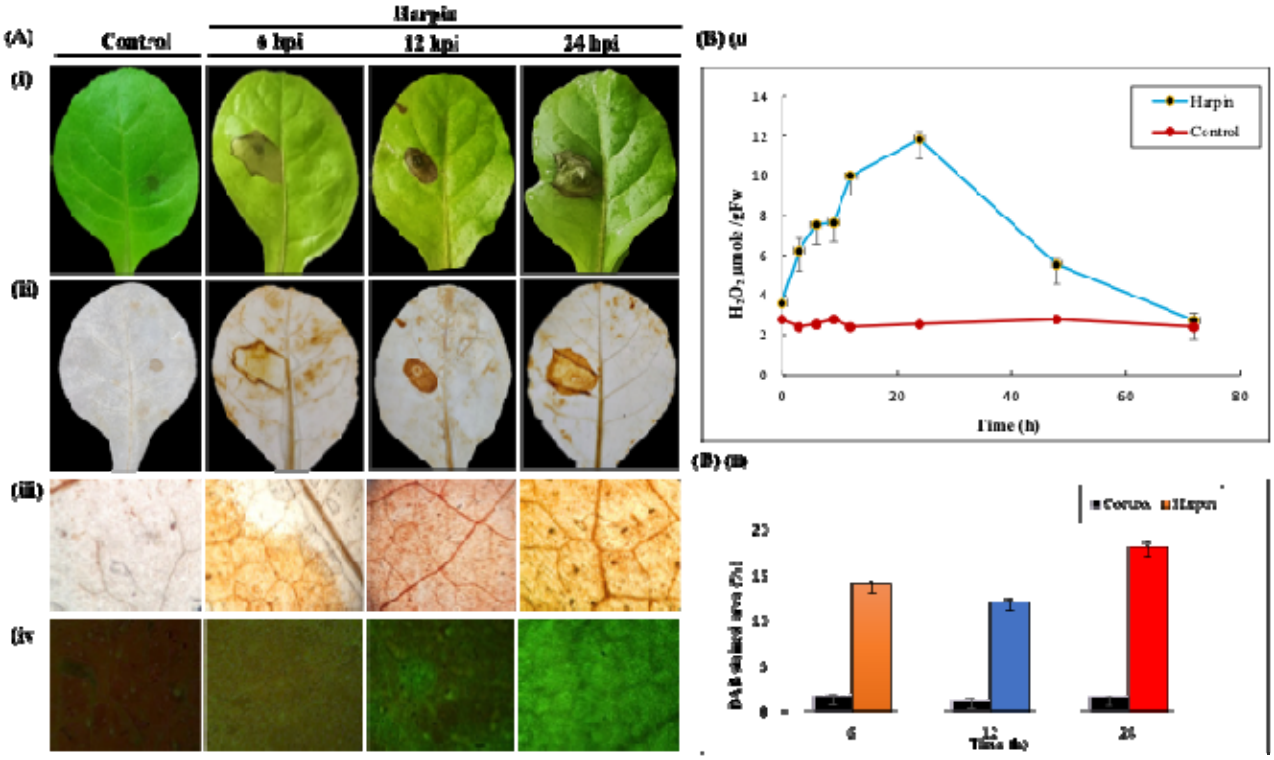

Figure 9. Histochemical observation and quantification of H_2O_2. (A) DAB staining (i = before bleaching, ii = after bleaching, iii = microscopic view) and (iv) DCFDA staining in *Nicotiana tabacum* leaves after 24 hours of infiltration with harpin (30 ug) and buffer (control). B (i = H_2O_2 quantification, ii = DAB-stained area (%)). The quantification of hydrogen peroxide by FOX reagent method. The x-axis shows the H_2O_2 content (uM/gFW) and DAB-stained area (%) in B (i) and B (ii) respectively, whereas the y-axis represented time (h) in both.

This is a provisional file, not the final typeset article

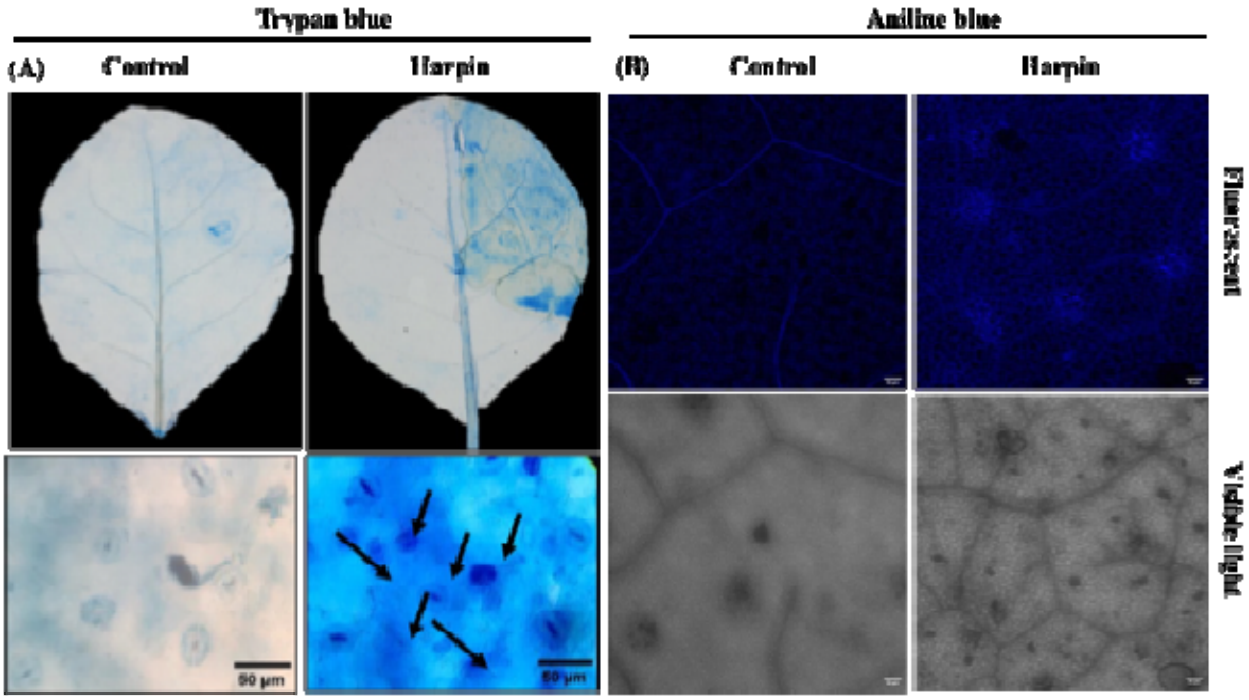

Fig. 10: Cell Death phenotypes and callose detection in leaves of *Nicotiana tabacum* in response to harpin infiltration observed by light and fluorescence microscopy. (A) upper panel shows pictures of full leaves infiltrated with buffer and harpin respectively while the lower panel shows light microscopy images of excised sections of the infiltrated region of leaves with HR development (3 dpi). Microscopic images (at lower panel) of HR phenotypes corresponding to hypersensitive cell death in harpin infiltrated leaves stained blue (marked with black arrows) at 3 dpi while there is no blue stain (cell death) observed in the control leaves. (B) Fluorescence microscopy images showing callose deposition in *Nicotiana tabacum* leaves in response to harpin protein after aniline blue staining. Leaves of *Nicotiana tabacum* observed at 24 hpi after infiltration with harpin (30 µg/ml) in 10 mM sodium phosphate buffer pH 7.5. As control, the same buffer was infiltrated on the left part of the leaves. Images are representative of three independent experiments using at least three leaves per experiment.

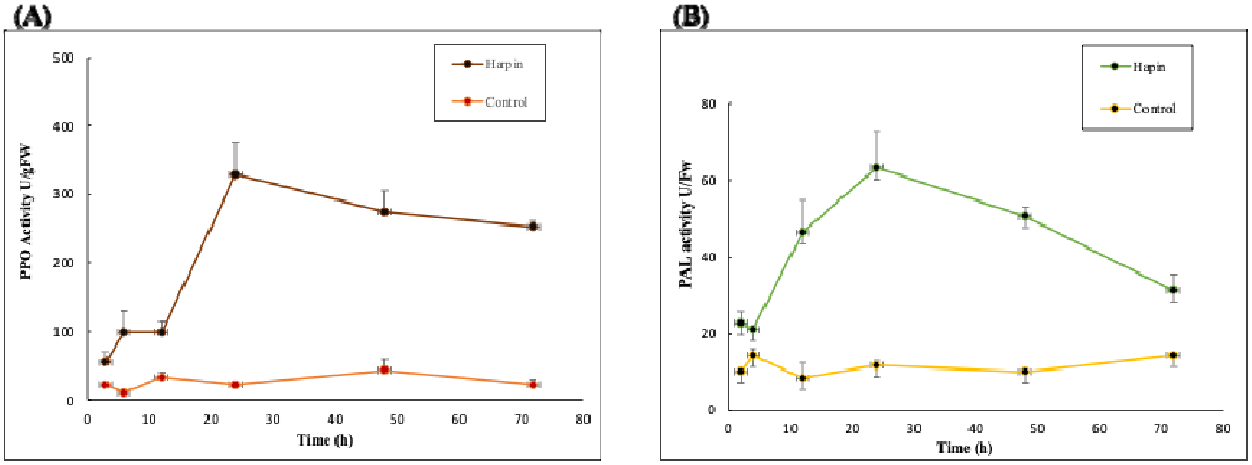

Fig. 11: Effect of harpin on the activities of defense-related enzymes in *Nicotiana tabacum*. (A) Polyphenol oxidase (PPO), a defense enzyme linked to pathogenesis, and (B) Phenylalanine ammonia-lyase, a defense enzyme linked to pathogenesis, both exhibited an increased activity post harpin (30 µg ml^{-1}) infiltration in tobacco leaves. The sodium phosphate buffer was used as control. The enzyme activities were measured 24 hours after infiltration by collecting the treated leaves. The findings displayed are the averages ± standard errors of three replicates (3 plants in each experiment).

This is a provisional file, not the final typeset article

Table 1:

S. No.	Physicochemical Properties	Values
1	Molecular weight	34.5 kDa
2	Number of amino acid residues	342
3	Theoretical pI	4.15
4	Molecular formula	$C_{1471}H_{2401}N_{415}O_{525}S_{9}$
5	Instability index	35.97
6	Extinction coefficient	5500
7	Number of negatively charged residues: Glu (D) & Asp (E)	42
8	Number of positively charged residues: Arg (R) & Lys (K)	19
9	Aliphatic index	85.99
10	Grand average of hydrophobicity (GRAVY)	-0.214

Physicochemical properties of harpin (HrpZ2), as determined with ProtParam tool.

Table 2: List of amino acid-level differences between two harpins ($HrpZ_{Pss}$ *vs* HrpZ2).

Sl. No.	**Harpin ($HrpZ_{Pss}$)**		**Harpin (HrpZ2)**		**Type of annotation**
	Position	Residue	Position	Residue	
1	25	Alanine (A)	25	Threonine (T)	Substitution
2	30	Serine (S)	30	Alanine (A)	Substitution
3	—	—	***Extra at 30***	Alanine (A)	Insertion in HrpZ2
4	102	Serine (S)	103	Asparagine (N)	Substitution and a shift due to

This is a provisional file, not the final typeset article

					insertion
5	117	Asparagine (N)	118	Serine (S)	Substitution and a shift due to insertion
6	135	Threonine (T)	136	Alanine (A)	Substitution and a shift due to insertion
7	226	Methionine (M)	227	Threonine (T)	Substitution and a shift due to insertion
8	243	Threonine (T)	244	Serine (S)	Substitution and a shift due to insertion
9	244	Arginine (R)	245	Serine (S)	Substitution and a shift due to insertion